

1-1-2017

Micromechanical Modeling of Shear Banding in Granular Media

Charles Clayton Goodman

Follow this and additional works at: <https://scholarsjunction.msstate.edu/td>

Recommended Citation

Goodman, Charles Clayton, "Micromechanical Modeling of Shear Banding in Granular Media" (2017).
Theses and Dissertations. 3089.
<https://scholarsjunction.msstate.edu/td/3089>

This Graduate Thesis - Open Access is brought to you for free and open access by the Theses and Dissertations at Scholars Junction. It has been accepted for inclusion in Theses and Dissertations by an authorized administrator of Scholars Junction. For more information, please contact scholcomm@msstate.libanswers.com.

Micromechanical modeling of shear banding in granular media

By

Charles Clayton Goodman

A Thesis
Submitted to the Faculty of
Mississippi State University
in Partial Fulfillment of the Requirements
for the Degree of Master of Science
in Civil Engineering
in the Department of Civil and Environmental Engineering

Mississippi State, Mississippi

December 2017

Copyright by
Charles Clayton Goodman
2017

Micromechanical modeling of shear banding in granular media

By

Charles Clayton Goodman

Approved:

Farshid Vahedifard
(Major Professor)

John F. Peters
(Committee Member)

Tonya Stone
(Committee Member)

Shantia Yarahmadian
(Committee Member)

James L. Martin
(Graduate Coordinator)

Jason M. Keith
Dean
Bagley College of Engineering

Name: Charles Clayton Goodman

Date of Degree: December 9, 2017

Institution: Mississippi State University

Major Field: Civil Engineering

Major Professor: Dr. Farshid Vahedifard

Title of Study: Micromechanical modeling of shear banding in granular media

Pages in Study: 66

Candidate for Degree of Master of Science

Shear banding is a commonly observed yet complex form of instability in granular media by which the deformation is localized in a narrow zone along a certain path. The aim of this study is to investigate the micromechanics of shear banding using the discrete element method (DEM). For this purpose, a model was developed and calibrated to simulate the macroscale behavior of sand under plane strain conditions. Upon validation against laboratory experiments, two types of confining boundaries, displacement- and force-controlled, were examined to study the kinematics of shear bands. A constant volume test was then used to investigate the evolution of antisymmetric stresses before, during, and after shear band formation. The results indicate that the antisymmetric stresses significantly increase within the shear band throughout the loading history, but may not describe the precursory shear band conditions. The DEM model is shown to properly capture the micromechanics of shear bands.

DEDICATION

To my wife Mary Evelyn Goodman. Your love is a gift from God and is undeniable evidence of His graciousness to me. Thank you for your constant love, support, and friendship.

ACKNOWLEDGEMENTS

I gratefully acknowledge the support of my advisor, Dr. Farshid Vahedifard who has pushed and encouraged me to be the best I can be. I am very grateful for your guidance, friendship, and the financial support that you secured for me. Also, I would like to thank my committee members. Dr. John F. Peters: your relentless dedication to excellence inspires me. Thank you in advance for patiently re-explaining to me all of the concepts that we have previously discussed. Dr. Shantia Yarahmadian: for sharing your contagious appreciation for mathematics with me. Dr. Tonya Stone: for your insight and expertise in micromechanics and DEM. Thank you all for guiding me through this process.

I would also like to thank Dr. Bohumir Jelinek for the countless hours you have helped me running my simulations and using HPC. There is no way this thesis would have been possible without you. Also, a very special thanks to my colleagues/friends past and present: grad school would not be nearly as enjoyable without your help and companionship. Thank you, Jonathan, Shahriar, Firas, Sannith, James, Kimia, Daniel, Toan, Nima, Syed, Jody, Mohammed, and Sona.

Finally, I would like to say a special thank you to my parents, Bart and Sandy, and my siblings, Lucas and Shaina, for providing me with irreplaceable childhood memories, and love and support the whole way through and still to this day. Also, to the

rest of my family (too many to name) for the unqualified support you have given me over the years.

TABLE OF CONTENTS

DEDICATION	ii
ACKNOWLEDGEMENTS	iii
LIST OF TABLES	vii
LIST OF FIGURES	viii
CHAPTER	
I. INTRODUCTION	1
Introduction and Background	1
Objectives	2
Scope and Contribution	2
II. BACKGROUND	6
Introduction	6
Historical Development	7
Continuum Bifurcation Theory	10
Micromechanics	12
III. KINEMATICS OF SHEAR BANDS IN PLANE STRAIN DEM SIMULATIONS	16
Introduction	16
DEM for Studying Shear Bands in Soil	17
Materials and Methods	19
DEM Calibration	22
Simulation Results	24
Effects of Boundary Conditions	28
Conclusions	30
IV. INVESTIGATING THE ROLE OF ANTISYMMETRIC STRESSES IN SHEAR BAND EVOLUTION	31
Introduction	31
Identification of Shear Banding in Granular Media	33
Continuum Properties and DEM	36

The Asymmetry of the Stress Tensor	36
DEM Formulation	39
Methodology.....	43
Results and Discussion	45
Conclusions	56
V. CONCLUSIONS.....	57
Summary of Findings	57
Recommendations for Further Research	58
REFERENCES	60

LIST OF TABLES

3.1 Properties and Values Used in the DEM Simulations.....	20
4.1 Bridging the scales: DEM and Cosserat Continuum.....	42

LIST OF FIGURES

1.1	Work flow	4
2.1	Early figures in the study of frictional media	9
2.2	Multiscale nature of granular media	13
3.1	Soft-sphere approach to DEM.	18
3.2	The reference assembly	20
3.3	Rolling friction calibration	23
3.4	Sliding friction calibration.....	23
3.5	Displacement-controlled simulation stress – strain behavior.....	26
3.6	Force-controlled simulation stress – strain behavior.....	26
3.7	Visualizations of shear bands for each simulation.....	27
3.8	Effects of rigid boundaries.....	29
4.1	Common shear band patterns.....	34
4.2	Observing shear band onset and patterns using the grid method.....	35
4.3	Particle contacts illustration for stress calculations.....	42
4.4	Distribution of particle sizes	43
4.5	The three cases examined.	45
4.6	Shear band pattern and rolling resistance.....	46
4.7	Stress – strain curve for the constant volume simulation	47
4.8	Angular velocity.....	48
4.9	Average angular velocity for all three cases	49

4.10 Particle contact moments	50
4.11 Average contact moments for all three cases.....	51
4.12 Antisymmetric stresses	52
4.13 Average antisymmetric stress for all three cases	53
4.14 Local porosity.....	54
4.15 Average local porosity throughout the simulation.....	55

CHAPTER I

INTRODUCTION

Introduction and Background

Copious amounts of research have been performed to better understand strain localization in granular materials, and it remains a prevalent topic today (e.g., see Bardet 1990 and Radjai et al 2017 for good review articles). Strain localization in granular media, often called shear bands, form under various loading conditions, and are generally associated with the failure of the material (Shi et al. 1999, Wang and Lade 2001, Wang et al. 2016). Although much research has been done and important discoveries have been made, there remains much to learn about this form of instability. For example, what conditions precede shear band formation? How can we mathematically define those conditions? How can we tie our understanding of the micromechanics of shear bands into existing continuum models? These are all questions that remain to be addressed.

Extensive work has been done on shear banding in granular media, yet mostly in two dimensions, and in a qualitative manner. The complexity of soil as an engineering material lies in its micro-structure. Soil is naturally an inhomogeneous, anisotropic, and elastic/plastic material which makes it difficult to predict its response to various types of loading (Zhao and Guo 2013, Loukidis and Ygeionomaki 2017). The relationship between the micro and macro scale response of a particulate material is not completely understood. Modern understanding of soil behavior has primarily been developed within

a continuum mechanics framework, which require very complex constitutive models to apply to granular materials (O’Sullivan, 2011). The discrete element method (DEM), originally proposed by Cundall and Strack (1979), is a numerical tool that can provide insight to individual particle interaction as well as the macro response of an assembly of particles. DEM has been utilized to model a wide variety of engineering applications including shear band development. A few recent examples include laboratory testing of granular media (Belheine et al. 2009, Guo and Zhao 2016) and micromechanical analysis of soils (Ngo et al. 2016, Geer et al. 2017) including the localization of deformation that takes place.

Objectives

The aim of this study is to investigate the micromechanics of shear banding using DEM. The main objectives of this thesis include a.) to investigate the effect of confining boundary conditions on the kinematics of shear bands, and b.) to examine the evolution of antisymmetric stresses and related variables before, during, and after shear band formation. The findings can provide further insight to the shear banding condition leading to an improved understanding regarding strain localization and failure in granular media.

Scope and Contribution

To achieve the given objectives, a DEM model is developed and calibrated to simulate the macroscale behavior of dry sand under plane strain conditions. Upon validation against laboratory experiments, two types of confining boundaries, displacement- and force-controlled, were examined to study the kinematics of shear bands. The displacement-controlled model is then used to investigate the evolution of

antisymmetric stresses before, during, and after shear band formation. The DEM model is used to observe how the variables in a shear band evolve with time under certain conditions.

The novelty of this work comes from a philosophy for understanding shear banding from a perspective of order. From previous works, it is understood that the conditions for the shear band to develop come early in the loading history before the shear band is visible (e.g., Wolf et al. 2003, Peters and Walizer 2013, Tordesillas et al. 2014). This was shown by Peters and Walizer (2013) who observe that when the affine motion is subtracted from the total deformation, you are left with patterns (swirl fields) that match the symmetry of the shear bands formed in the simulations. These patterns are visible early in the loading history, which indicates that shear band formation may be the result of an ordered phenomenon that develops gradually throughout loading rather than as a sudden bifurcation.

It is worth noting that spherical particles are used in this thesis as a mathematically simplified version of real soil. Also, these particles are not meant to be accurate depictions of the particles themselves, but to behave in such a way as to represent the behavior of actual particles well. In DEM studies particles are often much larger, and less in number than would be expected in a laboratory test, but similitude is obtained through dimensional analysis and calibration (Horner and Peters 2000, Coetzee 2016, Rackl and Hanley 2017).

In this thesis, chapter 2 presents and discusses the background information regarding shear banding in granular media. Special attention is paid to the continuum bifurcation theory and micromechanical approaches to solving shear banding problems.

The next portion of this work was performed in 2 phases (Figure 1.1), phase 1 being described in chapter 3, and phase 2 in chapter 4.

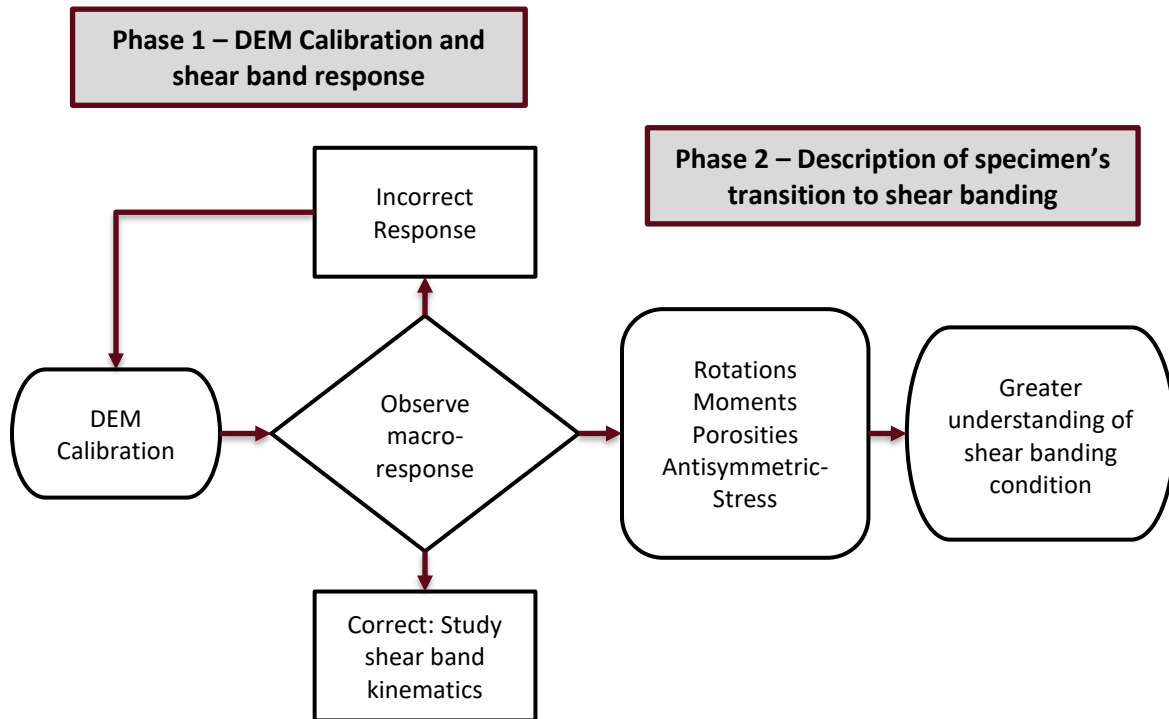


Figure 1.1 Work flow

The work in this thesis is performed in two phases as shown in the flow chart. Phase 1 consist of model validation using multiple loading schemes, and phase 2 involves studying the micromechanics of shear bands using continuum type measures.

In chapter 3, the initial DEM model is developed and presented, and the results for the calibration and kinematics of shear bands are discussed for two cases of confinement conditions: displacement- and stress-controlled. Chapter 4 discusses various methods used in the literature to identify shear band onset and evolution. Further, the formulation for the antisymmetric stress tensor is introduced as a potential identifier of shear band formation.

The effects of several variables including rotation, moments, porosity, and antisymmetric

stresses and their role in shear band formation are studied and discussed. Finally, in chapter 5, the summary and conclusions from the thesis, as well as recommendations for future research are presented.

CHAPTER II

BACKGROUND

A portion of chapter has been published as a conference article in Proc., Geotechnical Frontiers 2017: Geotechnical Materials, Modeling, and Testing, Geotechnical Special Publication No. 280, March 12-15, 2017, Orlando, FL, pp. 519-528. The original paper may be accessed at <http://dx.doi.org/10.1061/9780784480472.054>. Moreover, the paper has been reformatted and replicated herein with minor modifications in order to outfit the purposes of this thesis.

Introduction

Shear banding in soil is a form of instability in which deformation localizes into a narrow band during loading. Inside the shear band large plastic deformation occurs, while homogeneous deformation continues outside of the shear band. The onset of shear banding is generally associated with the beginning of failure for a material, where failure is considered to be the point in the stress-strain history when the material begins to experience excessive instability within a localized zone, and is no longer able to recover strength. This is not to be confused with other types of instability, such as liquefaction, where soil is destabilized by vibration and caused to behave like a fluid.

Within the field of geotechnical engineering, the study of shear bands is applicable to many problems. Problems that are characterized by a plane strain state (e.g., strip footings, levees, retaining walls, embankments, etc.) are often susceptible to this

type of instability. In slope stability and landslide analysis, the failure plane of a mass of mobilized soil is often considered a thin shear zone which could be modeled as a shear band (Donald and Chen 1997; Van Asch et al 2007; Laouafa and Darve 2002). Also, the shear banding is the primary mode of failure for off road vehicle mobility analysis of soil (Senatore et al. 2013, Maciejewski and Jarzebowski 2002, Senatore and Iagnemma 2014).

Shear banding in granular media has been widely studied in geotechnical engineering for the past 4 decades. For a topic so intensely researched, to make a small contribution regarding the understanding of shear bands in granular media is significant. In this chapter, an introduction is given to the problem of shear banding, and the background necessary to study the shear banding problem is presented. First, the motivation for studying shear bands in granular media and the historical overview of the topic is summarized in section 2.2. Sections 2.3 and 2.4 contain a discussion on the two major approaches to studying shear bands: continuum bifurcation theory, and micromechanical approaches. Finally, the basics of Cosserat theory is presented as a means of understanding micromechanics in continuum terms.

Historical Development

The study of shear banding emanates from the study of friction. Some of the earliest known scientific work on the study of frictional materials is that of Leonardo da Vinci (1452–1519). Hutchings (2016) notes that da Vinci is widely credited with defining the two fundamental principles of friction: 1) the force of friction between two surfaces is proportional to the load pressing the surfaces together, and 2) the force of friction is independent of the contact area between the two surfaces. Nearly 250 years later in 1773,

Coulomb, building on the work of his predecessors, laid the foundation for modern soil mechanics with his treatment of the “thrust of soil” behind a retained wall (Heyman 1972). He developed the formulation of the so-called Coulomb equation which, in its familiar form is expressed as,

$$|\tau| = c + \sigma \tan \phi, \quad (1.1)$$

where τ is the shear stress on the failure plane, σ is normal the stress, c is cohesion, and ϕ is the angle of internal friction. Equation (1) is the generalized form of Coulomb’s equation as expressed in the seminal work of Otto Mohr (1900). It is often referred to as the Mohr-Coulomb equation, although Mohr’s work was done without explicit reference to Coulomb (Vardoulakis and Sulem 1995). Since the work of Mohr (1900), strain localization in engineering mechanics has received a lot of attention. Figure 2.1 shows a sketch of the original figures used in Coulomb’s Essai (1773), and Mohr’s (1900) paper.

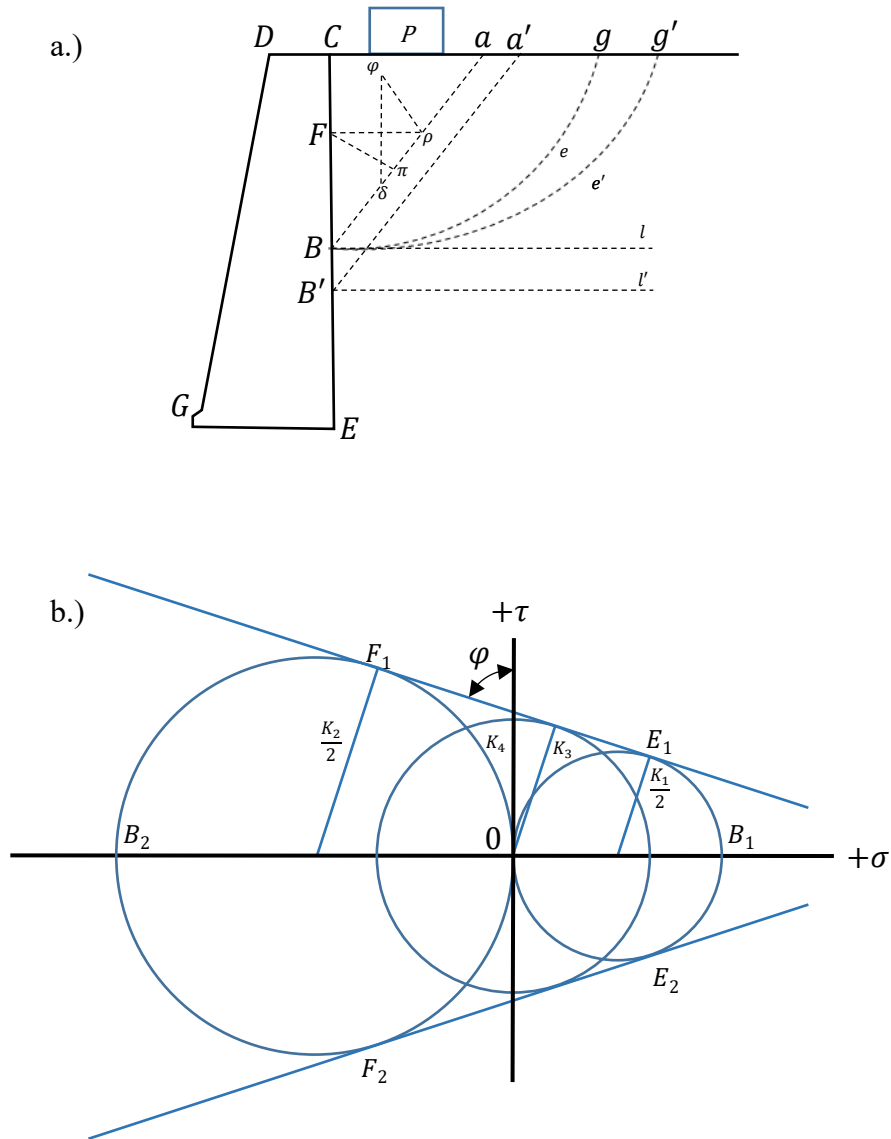


Figure 2.1 Early figures in the study of frictional media

A sketch of the original figures adapted from a.) the Coulomb (1773) retaining wall problem, and b.) Mohr's circle (from Mohr 1900).

The modeling and analysis of shear banding in engineering mechanics has fallen under two general categories: 1) continuum bifurcation theory and 2) micromechanical analysis. Historically, continuum methods have dominated the research, however, since

around the year 2000, micromechanical approaches have gained popularity due to improved imaging techniques and the advancement and availability of computational resources.

Continuum Bifurcation Theory

French mathematician Jacques Hadamard (1903) originally proposed a framework for mathematically describing strain localization in a continuum. Then, Thomas (1961) and Hill (1962) were among the first to further develop the strain localization theory for applications of “slip bands” in metals. Finally, Rice (1973) and Rudnicki and Rice (1975) developed the two-dimensional strain localization for geomaterials which sparked great interest from geotechnicians.

In general, three continuum approaches have been used to study the localization of plastic deformation due to shear banding in solids: wave propagation analysis (Hill, 1952, Thomas 1961, and Hill 1962), bifurcation analysis (Rudnicki and Rice 1975, Peters et al. 1988, and Vardoulakis and Sulem 1995), and uniqueness of solution (Valanis et al. 1993, Valanis and Peters 1996). An introduction of these approaches has been given by Rice (1976), and Valanis et al. (1993) show that all three approaches are essentially equivalent.

Of the aforementioned approaches, bifurcation analysis tends to be the dominant approach for describing shear bands in soil mechanics. In this case, shear banding is a form of bifurcation behavior in which the governing equations have two solution paths, one the “trivial” uniform strain solution and one the shear banding solution. In other words, shear bands appear in a material because of the bifurcation in the solution of the boundary value problem in which one solution yields linearly varying displacements from uniform strain,

and the second solution forms concentrated strains within an isolated surface (Peters et al. 1988). Rudnicki and Rice (1975), among others, give the theoretical framework for considering shear banding as a bifurcation problem. Their work shows that the failure plane of the shear band can be predicted from the constitutive equations. Rudnicki and Rice (1975) also show that the condition for shear banding does not necessarily coincide with the peak of the stress-strain curve (i.e., that the time of shear banding onset in the stress-strain history differed depending on the state of stress).

Vardoulakis et al. (1978) considered strain localization in biaxial tests on dry sand. This pioneering work of considering strength characteristics of sand as a bifurcation problem is based on an approach taken from studies on metal plasticity and rock mechanics. They found that the material response and loading configuration determine the bifurcation mode. They investigate the validity of the well-known Coulomb law and Roscoe solution for predicting the orientation of the slip surface in dry sand. Equation 1 shows the Coulomb law for predicting the orientation of a slip surface θ for a peak friction angle ϕ_p .

$$\theta = \pm \left(45^\circ + \frac{\phi_p}{2} \right) \quad (1.2)$$

The Roscoe solution defines the slip surface inclination as

$$\theta = \pm \left(45^\circ + \frac{\nu}{2} \right) \quad (1.3)$$

where ν (nu) is the angle of dilatancy as defined by the flow rule

$$\sin \nu = \frac{\dot{\epsilon}_1^{pl} + \dot{\epsilon}_2^{pl}}{\dot{\epsilon}_1^{pl} - \dot{\epsilon}_2^{pl}} \quad (1.4)$$

which assumes St. Vénant's rule of coaxiality for principal stresses and plastic strain rate. Their work shows that each of these solutions are valid for special cases, but the actual shear band inclination is extremely sensitive to the boundary condition and is not well

predicted by either model. Vardoulakis (1980) extend the Vardoulakis et al. (1978) work to show that theoretical solution of the shear band inclination could be better predicted by the geometrical mean of the classic Coulomb and Roscoe solutions.

Also, aimed at verifying some of the conclusions of Rudniki and Rice (1975), Peters et al. (1988) experimentally verified that the conditions for shear band formation depend on the stress conditions and occur at different points on the stress-strain curve depending on the test configuration. Their work compares the shear banding response of sand by comparing triaxial compression and extension, as well as plane strain compression tests. They found that the axisymmetric configuration is more stable than the plane strain configuration even after the onset of strain localization. Their findings also show that the localized instability cannot be adequately captured by the constitutive laws.

It is important to recognize the limitations of bifurcation analysis in regard to the traditional continuum approaches. Firstly, problems that involve large continuous deformations in soil mechanics are beyond the capabilities of numerical methods based on continuum mechanics. Important mechanisms that drive shear band behavior occur at the particle scale which requires knowledge of individual particle motion and continuum based models do not capture the kinematics of motion of a real soil system at the particle scale (Horner and Peters 2000). Among the issues at the particle scale are shear band thickness (Mühlhaus and Vardoulakis 1987; Tordesillas et al. 2004), granular diffusion, and the large deformations that occur.

Micromechanics

The approach considered in this thesis falls under the category of micromechanics. Micromechanics is the branch of soil mechanics that deals with

interparticle constituents in addition to the macroscale properties. The study of micromechanics is not meant to be a replacement for the past century of constitutive model development, rather it is a means of improving and informing those models by understanding the mechanisms that drive the constitutive behavior on the particle scale. Figure 2.2 presents a sketch of the relevant scales involved in the strain localization problem as defined in this thesis. There are the contact and particle scales from which we define how the granular material behaves at the system and macroscales. Next, there are the system/assembly and prototype scales, which would characterize the different scales found in laboratory testing. Finally, there is the field, structure, or macroscale.

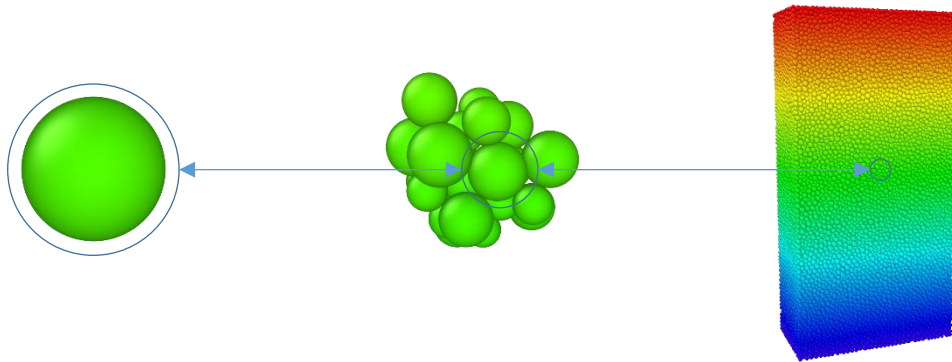


Figure 2.2 Multiscale nature of granular media

Problems in granular mechanics span multiple length scales from individual particles, to small clusters, to macroscale systems. An understanding of the mechanics on every scale is essential to solving instability problems.

The micromechanical approach to shear band research in the past has been mostly qualitative and in two dimensions. Early photoelastic visualizations (Wakabayashi 1950, Dantu 1957) and laboratory testing (Oda 1972, Oda et al. 1978) revealed the inhomogeneity and anisotropy of granular systems (Cundall and Strack 1979, Radjai et al. 2017). However,

soil fabric evolution and particle kinematics are very hard to quantify in 3D physical testing (Saadatfar et al. 2012). Brodu et al. (2015) use refractive index matching tomography to characterize microscopic characteristics of 3D granular packings. With this method, they are able to obtain contact force vector data while the system is deforming. This information can be used with other tomographic imaging techniques (e.g., microCT, and confocal microscopy) to better understand discontinuities in granular media (Brodu et al. 2015). However, it is still very difficult to use these techniques on soil due to the complex force network of the particle packings and the vast number of grains involved.

Perhaps the most promising tool for studying the micromechanics of granular materials is the discrete element method (DEM). Cundall and Strack (1979, 1983) developed the discrete element method (DEM), which revolutionized the study of granular media. DEM is a numerical tool that can provide insight to individual particle interactions as well as the macro response of an assembly of particles. For simple contact laws and calculation efficiency, it is common to use spherical particles to model soil in DEM. It is key to understand that, while spherical particles can be used to simulate realistic behavior, they are not able to replicate the micromechanics of real sand and have to be artificially calibrated to do so.

To account for the angularity and friction found in real soils, rolling resistance at particle contacts can be added for realistic behavior (Iwashita and Oda 1998). This type of study has given key insight to the micromechanics of shear bands. Iwashita and Oda (2000) show how particles under a load are arranged into force chains that carry most of the stress in the assembly. Under further loading the micro-structure becomes increasingly anisotropic, resulting in the breakdown of the force chains which cause instability (shear

bands). Following the intense strain softening, a new micro-structure is developed and a stable residual state is reached (Iwashita and Oda 2000). This behavior is experimentally verified in laboratory tests, and is also discussed in this study.

With modern laboratory data and understanding of soil behavior, it is possible to develop a DEM model that is able to analyze a large continuum of soil-like particles at the individual particle level. Thus, more accurate constitutive models can be developed for practical implementation which is one of the primary objectives of this research: to develop a realistic method of simulating soils such that the information provided at the discrete scale can fuel the understanding of engineering behavior at the prototype and macro scales. One of the potential ways of bridging the gap between discrete and continuum models is the use of a micro-polar continuum theory like Cosserat theory, which is introduced in chapter 4 of this thesis.

CHAPTER III

KINEMATICS OF SHEAR BANDS IN PLANE STRAIN DEM SIMULATIONS

“Portions of this chapter have been published as a conference article in Proc., Geotechnical Frontiers 2017: Geotechnical Materials, Modeling, and Testing, Geotechnical Special Publication No. 280, March 12-15, 2017, Orlando, FL, pp. 519-528. The original paper may be accessed at <http://dx.doi.org/10.1061/9780784480472.054>. Furthermore, the paper has been reformatted and replicated herein with minor modifications in order to outfit the purposes of this thesis.”

Introduction

Extensive experimental and analytical studies have been performed in the past 40 years to describe the mechanics of shear banding in granular materials and to explore the robustness of related numerical models. Advances in laboratory imaging, coupled with the use of the discrete element method (DEM) to simulate particle systems, combined with new statistical methods based on network theory has given the key steps in discovering the evolution of the shear localization process.

The mechanics of shear bands have been studied extensively both experimentally and analytically, yet mostly in a qualitative manner and in two-dimensions. The evolution of the micro-deformation mechanism leading to the development of shear bands is still not well understood and has important implications in three-dimensional analysis.

Presented herein is a promising method of modeling the micromechanics of the shear

band phenomenon in plane strain using parallelized discrete element method (DEM). The preliminary results show the DEM's capability of responding correctly to different loading conditions giving an accurate depiction of the behavior of real soil. The preliminary results from the DEM simulations are presented and discussed.

The purpose of this study is to qualitatively capture the kinematics of shear bands using a three-dimensional discrete element model in plane strain. The greater vision of this work is to provide a functional model capable of handling large systems using high performance computing, with an aim towards either modeling prototype scale experiments with high microscale resolution and a sufficiently large domain. First, a discussion on the discrete element method (DEM) as a capable tool for this task is presented. Next, the results from parallelized DEM plane strain tests are presented for systems under two different loading mechanisms. Each loading condition results in a well-defined and unique shear band proving the validity of the model. This provides a means of extending the plethora of work done using two dimensional systems of discs, into three dimensional studies which are more limited.

DEM for Studying Shear Bands in Soil

DEM, originally developed by Cundall and Strack (1979) for granular mechanics, is a numerical tool that can provide insight to individual particle interactions as well as the macro response of an assembly of particles. DEM explicitly considers the motions and forces of individual particles, which makes it an appropriate candidate for modelling granular media, such as soil, at length scales where the material does not behave as a continuum.

In DEM particles are represented by geometrically simple idealizations of the natural granular material such as soil. Spheres, ellipsoids, and combinations of spheres and ellipsoids are commonly used because of their simply geometry. The particles move by either translation, rotation, or a combination of the two. The position of the particles in DEM are calculated by integrating Newton's second law for linear and angular momentum, $F = ma$ and $\tau = I\alpha$, where F is the force vector, m is the mass, and a is acceleration associated with each particle; τ is the net external torque on the particle, I is the moment of inertia, and α the angular acceleration. The movement of each particle is defined by 6 kinematic variables, 3 linear velocity components, and 3 rotational velocity components. Depending on the particle geometry (spheres in this case), the contacts of particles with other particles are calculated by an idealized overlapping called the soft-sphere approach (Figure 3.1).

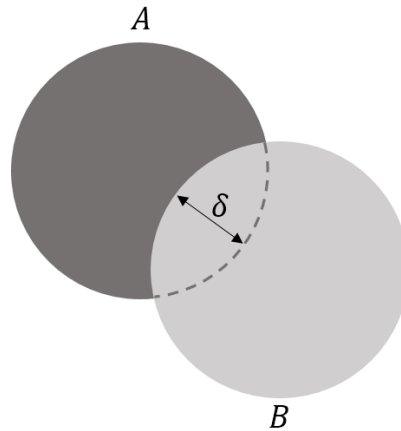


Figure 3.1 Soft-sphere approach to DEM.

Illustration of the soft sphere approach by which inter-particle forces and moments between particles A and B are calculated as a function of particle overlap, δ , at the contacts

Actual particles deform when they come into contact with each other, but the particles in DEM are allowed to overlap, and this overlap defines the force and moment associated with the contact. The positions of the particles for the next instance of time are computed using explicit time integration. That is, the particle location in the next time step depends only on the current configuration.

Materials and Methods

The plane strain simulations performed in this initial phase of the study were carried out using a three-dimensional discrete element code developed via collaboration between the US Army Corps of Engineers Research and Development Center (ERDC) in Vicksburg, MS and Mississippi State University. The code is useful for a variety of engineering applications, and is capable of simulating various geotechnical laboratory tests. The plane strain configuration was chosen for two main reasons. First, this configuration lends itself to many naturally occurring situations of interest to geotechnical engineers (e.g., levees, dams, retaining walls, strip footings, etc.). Second, the plane strain apparatus is a three-dimensional test that produces nominal two-dimensional deformation (yet with 3-D particle motion). Thus, highly visible shear bands are produced across the plane strain face. The research presented here will focus on the implications of the latter reason.

The plane strain simulations performed in this study employ a strain rate controlled test that uses velocity driven walls. The effects of loading conditions on shear band formation was investigated using a granular assembly consisting of smooth unbonded spherical particles whose properties are summarized in Table 3.1. The particles are bound by frictionless rigid platens that do not interact with each other during the

consolidation and loading processes. The soil particle contact forces are computed from simple binary models involving springs, dashpots, and frictional sliders. The acceleration, velocity and displacement of the particles are then calculated according to Newton's laws of motion. The mathematical details of the code and DEM in general can be found in the literature (Carrillo et al. 1996; Horner et al. 2001; Walsh et al. 2007).

Table 3.1 Properties and Values Used in the DEM Simulations

Property	Units	Value
Number of particles	–	64,000
Maximum radius	m	0.010
Minimum radius	m	0.005
Normal stiffness	kN/m	245.18
Shear stiffness	kN/m	87.56
Contact friction (sliding)	–	0.50
Contact friction (rolling)	N-m	0.01
Initial specimen height, z	m	0.60
Initial specimen width, y	m	0.30
Initial specimen thickness, x	m	0.15
Initial area porosity	–	0.364
Specific gravity	–	2.65

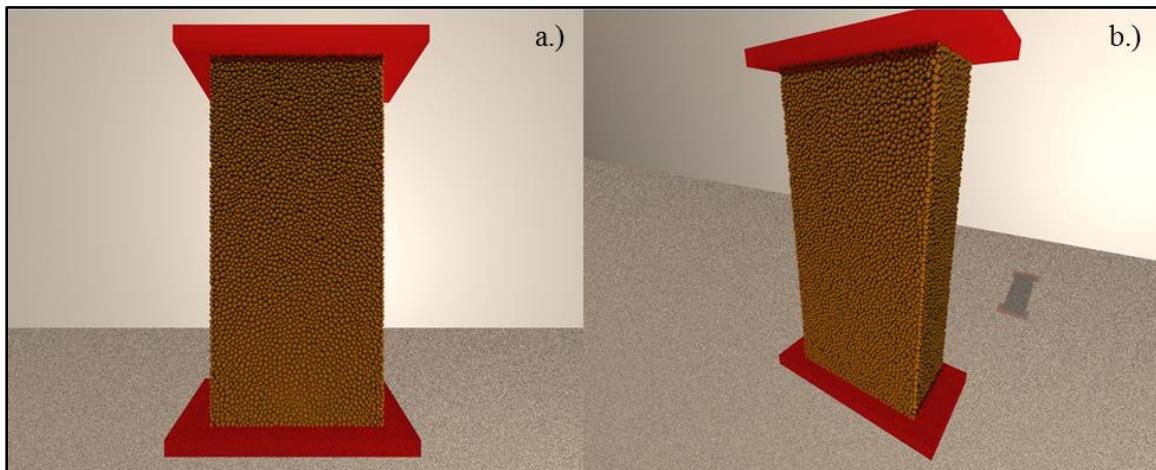


Figure 3.2 The reference assembly

64,000 particles initial reference assembly shown in a.) the front view (x facing) and b.) a perspective view. Plane strain and confining platens not shown for clarity.

The particle assemblies were generated in a loose initial configuration in which no particles were touching. Without the bias of gravity, the particles were slowly consolidated without friction by applying velocities to the bounding platens until the desired confining pressure (55 kPa) was reached. This final initial packing, referred to from here on as the reference assembly (Figure 3.2), was used for each simulation.

For the initial phase of the study, the simulation size was restricted to 64,000 particles representing an assemblage of approximately $20 \times 40 \times 80D_{50}$ which is large enough to capture important shear band characteristics and macroscale behavior. The initial consolidation is stopped when the specimen reaches an internal confining pressure of approximately 55 kPa. The z axis is the vertical direction, x the direction of zero strain, and y the direction of lateral strain. The x dimension is equal to half of the y dimension. Deformation of the reference assembly was controlled in two ways: displacement driven confining boundaries or strain controlled, and force driven confining boundaries.

The first type of test, referred to as the displacement-controlled test, the boundaries are velocity driven, and thus deformation is controlled by a constant strain rate. This test is approximately constant volume. In the second type of test the boundaries are controlled using a constant force and is referred to as the force-controlled test. For the displacement-controlled tests, the particles were confined by the rigid platens lengthening in the y dimension which held the particles at a near constant confining pressure in the y direction and in a state of near-constant volume. For the force driven boundary condition, the reference assembly was confined using a constant force applied to the y platens. For this loading condition, the force remained constant causing the particles to steadily increase in confining pressure until instability visually occurred. During loading, the z

dimension was reduced at an equal and constant rate from the bottom of the assembly for both types of test.

DEM Calibration

The method used to calibrate the model was to adjust micro-scale parameters that govern the macro-scale behavior, until a suitable match with macro-scale behavior is obtained. This is done so that the model is capable of solving problems across multiple spatial scales while honoring the natural kinematics of the particles. The goal is not necessarily to achieve realistic particle size or shape, rather it is to achieve realistic particle-scale and system-scale behavior.

For model calibration, it was found that inter-particle rolling friction (Figure 3.3) and sliding friction (Figure 3.4) had the most profound effect on the stress-strain behavior of the system. A parametric study was performed where these friction parameters were varied until stress-strain behavior similar to that of laboratory plane strain tests on sand was achieved (Alshibli and Sture 2000). The properties listed in the aforementioned Table 3.1 were found to be sufficient for achieving system level behavior as well as natural particle kinematics.

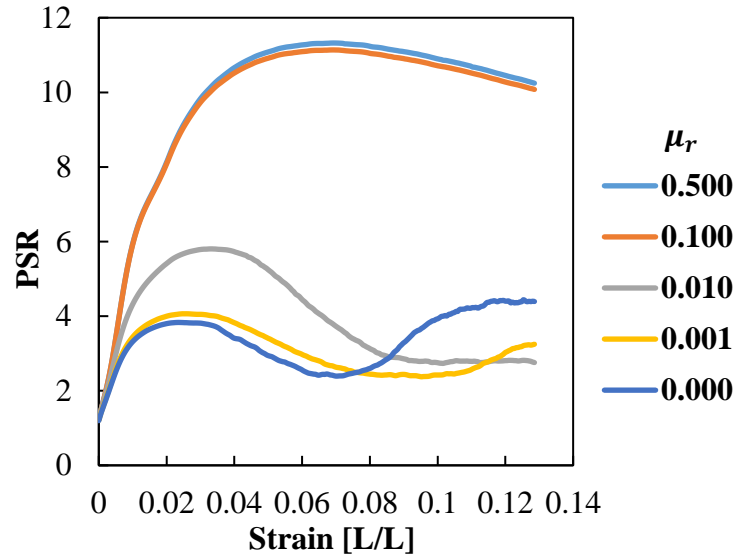


Figure 3.3 Rolling friction calibration

The effect of changing the rolling friction coefficient, μ_r , on the shape of the stress-strain curve where $\mu_s = 0.5$.

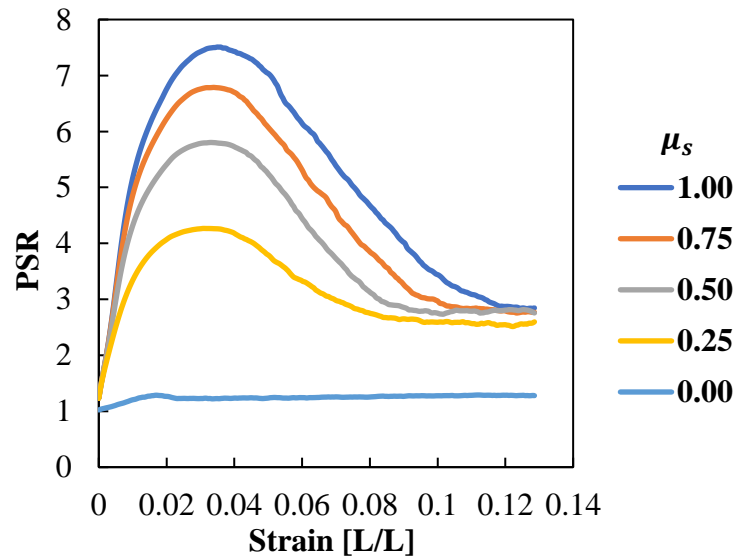


Figure 3.4 Sliding friction calibration

The effect of changing the sliding friction coefficient, μ_s , on the shape of the stress-strain curve where $\mu_r = 0.01$.

Figure 3.3 shows the profound impact that the rolling resistance has on the macroscale behavior of the system. However, once the proper shape of the stress strain curve is achieved with the rolling resistance, the overall strength of the system can be easily adjusted with small changes in the sliding friction (Figure 3.4). One thing to note is that the relationship between rolling and sliding friction to get a specified PSR is not unique, and should be coupled with another parameter such as the constant volume friction angle to get a unique pair.

Simulation Results

Plane strain tests were performed under two stress paths using the reference assembly discussed above. Figure 3.5 and Figure 3.6 show the stress-strain response of the assembly to displacement-controlled (velocity displaced) and force-controlled simulations, respectively. In each case the deforming system undergoes homogeneous deformation until, after a peak stress is reached, at which point a sharp drop in stress occurs. This softening is the result of material behavior inside the shear band where the particle kinematics is dominated by rotation and force-chain buckling.

The diamond symbol on the curves represent the point where shear localization becomes visually evident. At this point the particles organize the global specimen into two or more distinct sections as indicated visually by the coloring of the particles according to their velocity as shown in Figure 3.7. Figure 3.5 corresponds to the shear band shown in Figure 3.7a and 3.7b and Figure 3.6 corresponds to the shear band in Figure 3.7c and 3.7d. In each case shear banding begins near the peak of the stress-strain curve indicating that the intense softening occurs as a result of the instability. The shear bands initiated at 3.2% and 3.8% strain for the displacement-controlled and force-

controlled specimens, respectively. This result seems to be within reasonable agreement with similar laboratory experiments on sand (see Alshibli and Sture 2000).

The peak friction angles for each specimen was measured to be 45.6° for the strain controlled and 44.9° for the force controlled. According to the Coulomb theory stated above this should yield a slip angle of 67.8° and 67.5° for each case, respectively. The inclination of the shear bands was measured to be about 60° for each case at peak stress values. Thus, the Coulomb failure law for predicting the slip surface over predicts the inclination angle in the case of shear band formation in this granular assembly.

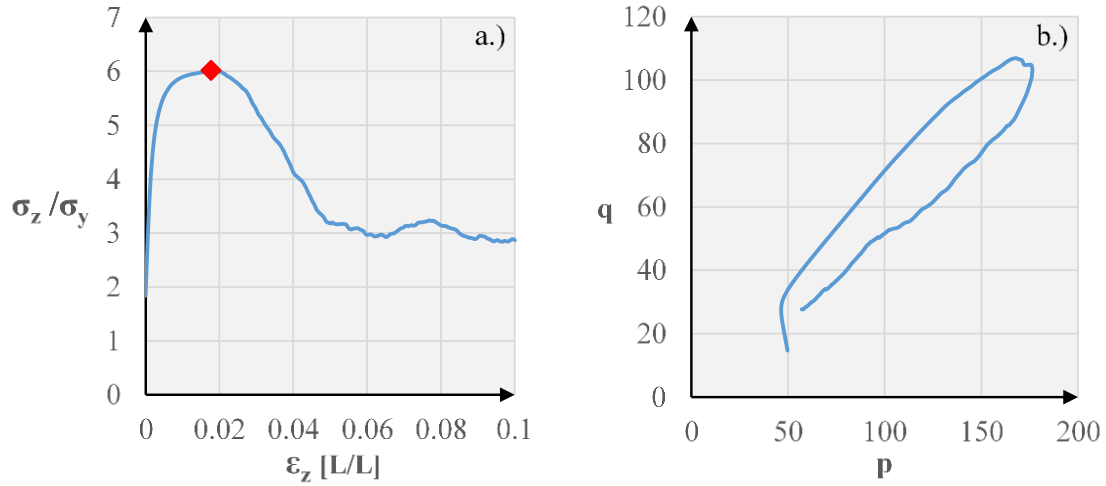


Figure 3.5 Displacement-controlled simulation stress – strain behavior

Displacement-controlled simulation showing a.) stress - strain behavior and b.) the stress path. The diamond symbol marks the onset of shear banding for each case.

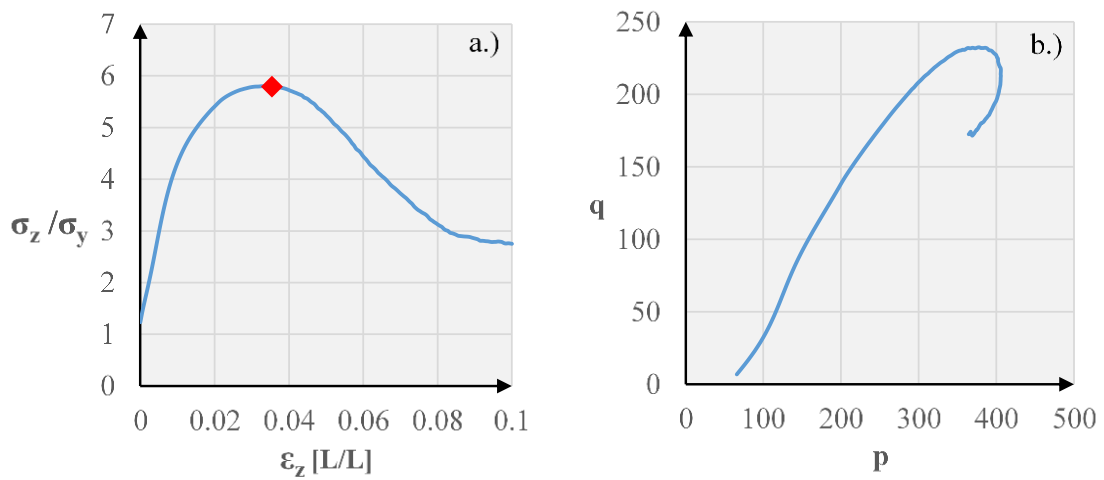


Figure 3.6 Force-controlled simulation stress – strain behavior

Force-controlled simulation showing a.) stress - strain behavior and b.) the stress path. The diamond symbol marks the onset of shear banding for each case.

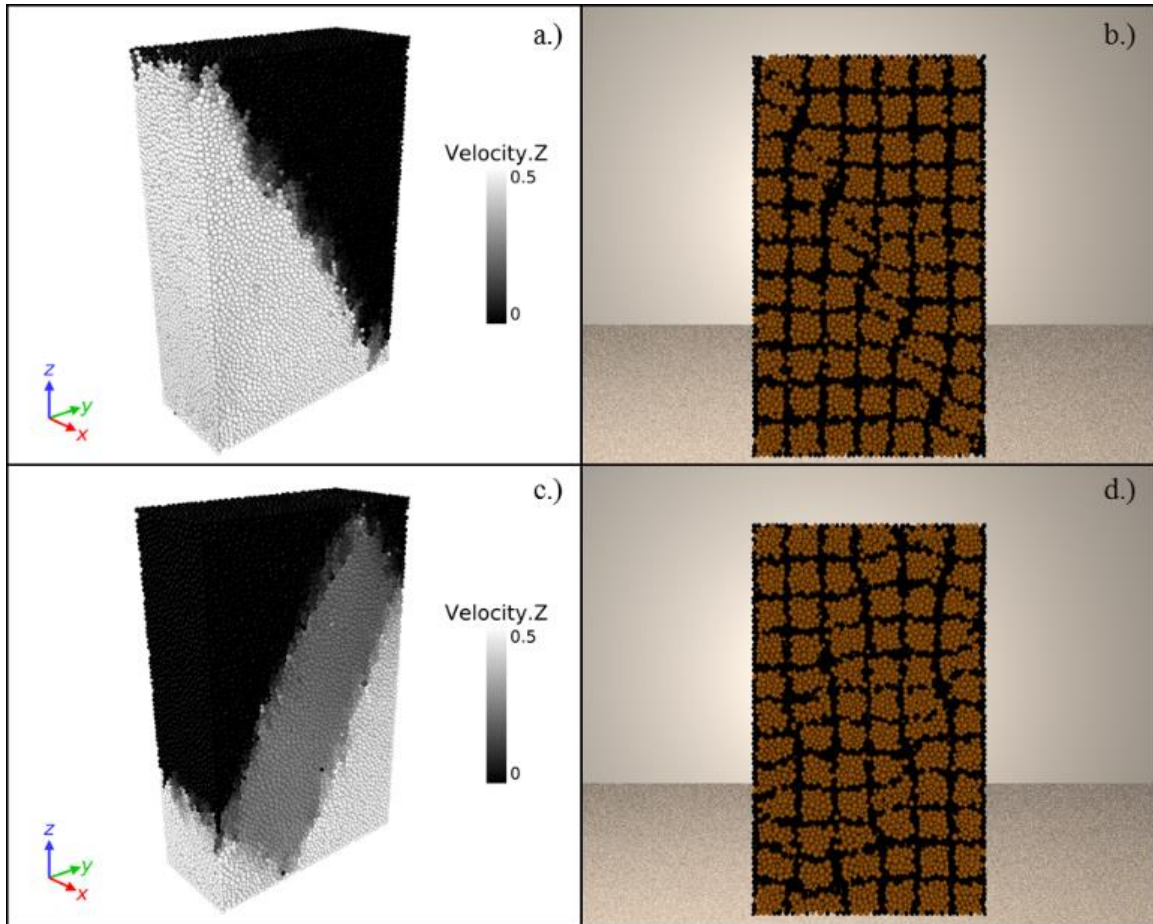


Figure 3.7 Visualizations of shear bands for each simulation

Parts a.) and b.) show two views and visualization types for the shear band in the displacement-controlled simulation, while c.) and d.) show the force-controlled.

In Figure 3.7, the grid lines clearly show the kinematic constraints imposed by the rigid boundary. Vertical lines inside the specimen clearly show the “buckling” deformation related to shear band formation, whereas those on the boundary remain straight, thus stabilizing an exterior rind of particles.

While the purpose of this study is to impose different loading regimes to the same reference assembly, it should be noted that the response is dependent on the initial configuration of the particles. Gu et al. (2014) used DEM to simulate drained biaxial tests

with different initial confining pressures and densities in an attempt to find the correlation between the occurrence of shear banding and evolution of the microstructure. They show that the loose state with high confining pressure delays the appearance of shear bands, and that the initial conditions also effect the anatomy of the shear band (e.g., higher density and higher confining pressures decrease shear band thickness and increase the inclination angle).

Effects of Boundary Conditions

Meeting the complex requirements of more sophisticated experiments involves a number of combinations of rigid and flexible boundary conditions. The effects of these boundary conditions are often overlooked because it is assumed that controlled stress and controlled displacement boundary conditions should give comparable results. However, there is evidence that the choice of boundary condition does impact results, most likely the result of the finite-sized particles that make up a granular domain. Several investigations are planned to evaluate this condition including using a membrane to produce flexible stress-controlled boundary conditions and reducing particle size relative to specimen dimension.

Laboratory tests performed on cubical specimens of both stiff and flexible boundaries show that specimens with stiff boundaries had greater stress-strain moduli, lower strain to failure ratios and higher strengths than those using flexible boundaries (Lade and Wang 2012 and Lade et al. 2014). This behavior is speculated to be attributed in part to the support of force chains along the boundaries due to the stiff platens. The particles line up along the plane of the platen, which allows them to have an exaggerated stiffness and resistance. In effect, the stiff platen provides support that promotes stability.

Similar findings appear in micro-mechanical research of particles being modeled using the discrete element method (DEM). Peters and Walizer (2013) observed that upon subtraction of the average uniform strain from the total deformation field in simulated two dimensional biaxial compression a background deformation of vortex-like flow patterns (swirls) are revealed. This background deformation field is controlled by the boundary conditions and can be shown to define the eventual shear localization pattern. The swirls result from the breaking down of force chains which releases kinetic energy into the system and drives particle diffusion. Figure 3.8 shows this behavior as well.

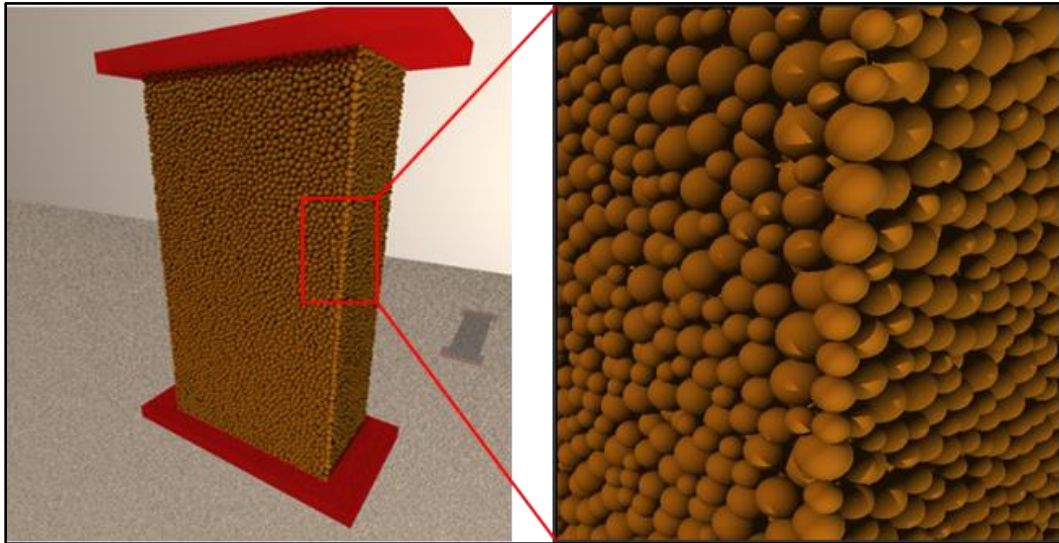


Figure 3.8 Effects of rigid boundaries

Particles beginning to line up in the corners forming platen – supported force chains capable of yielding higher than normal stresses at the boundaries.

The author is currently working on a method for testing the effects of this behavior by introducing a flexible membrane boundary condition, which will allow the particles move in a more natural way at the boundaries.

Conclusions

Continuum analysis will always be an important tool in soil mechanics and geotechnical engineering. However, many mechanisms that cause failure and instability in soil happen at the micro (granular) scale. Studying these phenomena and physically describing them is an important factor in improving the quality of continuum constitutive relationships. The discrete element method was employed to study the effects two types of laboratory loading conditions in plane strain. One condition was a displacement-controlled confining pressure and the other condition a forced-controlled confining pressure.

Preliminary results show that at variance with expectations for a theoretical continuum, the discrete material performs differently for displacement control versus stress control. This appears to be consistent with recent results for physical tests on sand. There is a close qualitative comparison between shear banding and load-deformation behavior that is similar to physical tests on sand. The DEM provides a detailed picture of the mechanisms controlling shear band evolution.

CHAPTER IV
INVESTIGATING THE ROLE OF ANTISYMMETRIC STRESSES IN SHEAR BAND
EVOLUTION

Introduction

Strain localization in the form of shear banding is a well-known issue in soil stability. Shear bands are commonly observed in geologic faults (Rice 2006, Marone and Kilgore 1993), laboratory testing of soils (Peters et al. 1988, Alshibli and Sture 2000, Sadrekarimi and Olson 2009), terramechanics (Senatore et al. 2013, Maciejewski and Jarzebowski 2002, Senatore and Iagnemma 2014), and many other applications in granular media. Studying the problem of shear banding is of great value because of the insight it will give to understanding and predicting the failure of a material. Shear banding occurs when the deformation of a material localizes into a thin zone. Inside the shear band large plastic deformation occurs, while homogeneous deformation continues outside of the shear band.

Stress in granular materials is primarily transferred through columns of individual particles called force chains (Majmudar and Behringer 2005). The buckling of these force chains, which occur on the particle scale, causes instability that leads to shear band development (Oda et al. 2004, Tordesillas and Muthuswamy 2009). This is of utmost importance in civil engineering where stress is a primary design factor for geotechnical structures. Upon loading, fabric anisotropies are induced which effect the materials

strength, stiffness, and permeability (Kuhn et al. 2015). These anisotropies can be effectively quantified and studied using micromechanical techniques such as DEM and digital imaging (Kuhn et. al. 2015, Majmudar and Behringer 2005). Other important micrometrical considerations in granular media include (but is not limited to) jamming (Majmudar et al. 2007, Tordesillas 2007), force transmission (Azéma et al. 2007), and particle diffusion (Ottino and Khakhar 2000), all of which have implications to modeling instability and shear banding.

In this study, plane strain discrete element simulations are used to collect data about shear band formation. The data include particle motions (velocity, acceleration, rotations, etc.), stresses, moments, contact forces, and number of contacts. Of particular interest is exploring the role of the antisymmetric stress tensor in shear banding. To do this, first, we will introduce the antisymmetric stress tensor and develop the reasoning for looking at it during shear band formation. Then, the plain strain DEM model used in this study is presented and discussed. Next, an exploratory data analysis including visualizations of the entire strain history of the simulations are presented. Finally, the results show that the antisymmetric stresses significantly increase within the shear band throughout the loading history, but may not describe the precursory shear band conditions as hypothesized.

The motivation behind the investigation of the antisymmetric stresses comes from the study of particle rotations (e.g., Bardet and Proubet 1991, Oda and Kazama 1998) which are observed in numerical simulations and physical laboratory tests of shear bands. If rotations occur, there must be moments that resist the rotations before they happen. It can be shown that these moments in DEM (the contact couples), when combined with the

moments caused by the intergranular forces, are scaled antisymmetric stresses (by a constant of volume), from which we get the motivation to study them as a characteristic of shear band behavior. However, relationship between the rotations and the antisymmetric stresses, and their evolution as shear banding proceeds, has not been explored.

Identification of Shear Banding in Granular Media

Generally, shear bands in granular media have been studied from the perspective of bifurcation analysis (Rudnicki and Rice 1975, Vardoulakis et al. 1978). A bifurcation is a form of instability where the solution to the governing equation bifurcates into two or more solution paths. In granular media, the so-called trivial solution to the constitutive equation is homogeneous deformation, and the bifurcation solution is the shear band. Understanding shear bands from this perspective has led to great advancements in the study of instabilities of granular materials. Yet, evidence from the study of nonaffine particle motion and vortices in numerical simulations (Peters and Walizer 2013, Tordesillas et al. 2014) shear banding can be understood as more of an emergent behavior that is present from the beginning of the solution.

In practice, shear bands are usually characterized by their orientation, θ , and the patterns that they form (see Figure 4.1). Desrues and Viggiani (2004) give a show a plethora of possible shear band patterns using stereophotogrammetry to measure deformations and strain fields in plane strain tests under a variety of initial conditions and that the shear band width and orientations do not fully describe the band throughout the entire test. Laboratory tests on physical sand report shear band orientations from approximately 45° to 70° under plane strain conditions (Vardoulakis et al. 1978, Alshibli

and Sture 2000). The large range of variation in the shear band inclinations are caused by material variability, differing initial conditions, loading regimes, and boundary conditions. Testing configuration, bedding planes, principal stress directions and other parameters are also known to cause variability in shear band patterns and orientations (Peters et al. 1988, Wang and Lade 2001. Lade et al. 2014).

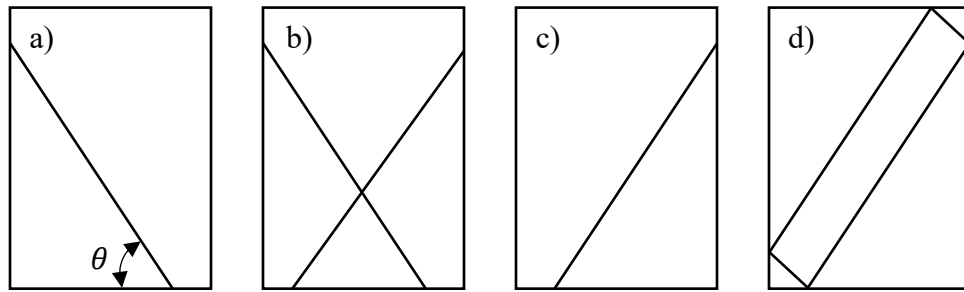


Figure 4.1 Common shear band patterns

a) Illustration of the shear band orientation, θ , and b) – d) common patterns observed in laboratory and numerical tests of soil.

Identifying shear band onset and evolution is generally done in a qualitative manner by imposing a grid on the membrane of the soil, and watching as the grid heterogeneously deforms along the shear band, and homogeneously deforms outside of the band. Figure 4.2 shows an illustration of how this is done using a physical plane strain specimen (from Alshibli and Sture (2000) and using a DEM visualization.

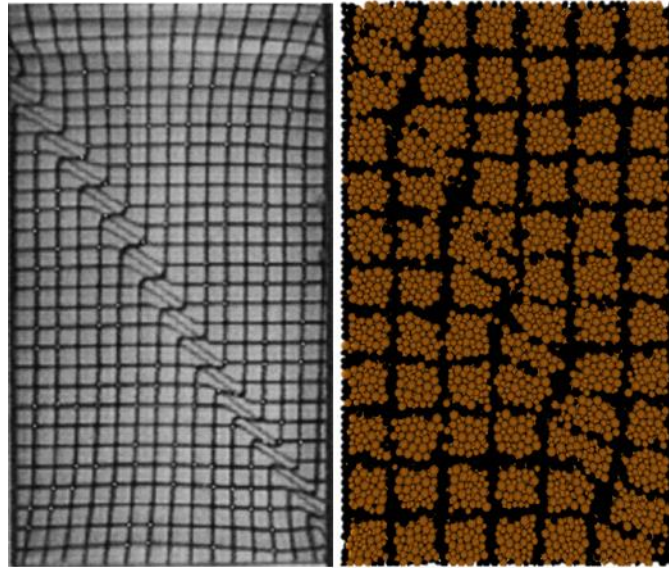


Figure 4.2 Observing shear band onset and patterns using the grid method

A side by side comparison of a similar shear banding pattern and how it is visualized with a superimposed grid in a physical plane strain specimen of sand (left - taken from Alshibli and Sture 2000) and a numerical DEM specimen (right).

Other methods of identifying shear bands in laboratory tests are photographic techniques such as the aforementioned stereophotogrammetry method (Desrues and Viggiani 2004), digital image correlation (Rechenmacher and Finno 2003, Rechenmacher 2005), and X-ray computed tomography (Batiste et al 2004, Alshibli and Hasan 2008). These methods are capable of taking images of the specimen over small time increments to measure the local displacement mechanisms involved in shear band initiation and evolution. While these techniques provide high-resolution data, other micromechanical techniques, such as DEM, are capable of providing information on the particle scale anywhere within the specimen (as opposed to only on the surface), which enables further analysis of the mechanisms that drive shear banding.

The micromechanics of shear bands are typically studied using imaging techniques and numerical simulations (e.g. Alonso-Marroquín and Vardoulakis 2005, Oda and Kazama 1998, Brodu et al. 2015, Zhou et al. 2017). Historically, most micromechanical studies have been done in two dimensions and in a qualitative manner. Recently, however, an outflux of research has been taking a more quantitative approach to understanding micromechanics by the examination of particle fabric evolution (Kuhn et al. 2015, Jing et al. 2017), particle crushing (Ma et al. 2016, Zhou et al. 2017), and other local particle statistics. A similar motivation in this study is applied to describing the behavior of shear banding. Micromechanical measures such as rotations, moments, and antisymmetric stresses are examined to quantify shear band motion before and during formation.

Continuum Properties and DEM

The Asymmetry of the Stress Tensor

The stress tensor, σ_{ij} , completely describes the state of stress at a point and is written in matrix form as

$$\sigma_{ij} = [\sigma] = \begin{bmatrix} \sigma_{11} & \sigma_{12} & \sigma_{13} \\ \sigma_{21} & \sigma_{22} & \sigma_{23} \\ \sigma_{31} & \sigma_{32} & \sigma_{33} \end{bmatrix}. \quad (3.1)$$

It can be decomposed into a symmetric part (using index notation),

$$\sigma_{ij}^s = \frac{1}{2}(\sigma_{ij} + \sigma_{ji}) \quad (3.2)$$

and an antisymmetric part,

$$\sigma_{ij}^a = \frac{1}{2}(\sigma_{ij} - \sigma_{ji}). \quad (3.3)$$

While the stress tensor can only be symmetric in a standard continuum, in DEM and Cosserat media, the antisymmetric part is non-zero. This asymmetry in the stress tensor is not a new concept in soil mechanics, but has been noted by several researchers (e.g., Bardet and Vardoulakis 2001, Tordesillas and Walsh 2002, Kuhn 2003, Goldhirsch 2010). However, understanding its role in shear band formation and evolution has not been explored.

A Cosserat continuum is one in which each material point is considered an infinitesimal rigid body. Cosserat theory is discussed in this thesis as a potential option for understanding DEM data in continuum terms. Localization of strain in granular media leads to a change in scale of the problem such that the phenomena occurring at the granular scale cannot be ignored in considering the macroscale behavior (Vardoulakis and Sulem, 1995). Thus, a theory that accounts for the micromechanics of a material, including particle rotation and shear band thickness, such as Cosserat theory, is needed. Cosserat theory is an extension of classical continuum mechanics in which additional kinematical (rotational) degrees of freedom are utilized. In a Cosserat media, each particle is individually characterized by a velocity vector and a rotation vector.

In traditional continuum mechanics, the general principles and laws that apply to the continuum are the locality of neighboring material points, conservation of mass, conservation of linear momentum, conservation of angular momentum, and the first and second laws of thermodynamics. It is from the balance of linear momentum that we arrive at the differential equations of equilibrium

$$\sigma_{ji,j} + \rho b_i = \rho \dot{v}_i \quad (3.4)$$

where $\sigma_{i,j}$ is the Cauchy stress tensor, ρb_i are body forces, and \dot{v}_i is the acceleration of the material point. The balance of angular momentum taken for an arbitrary volume (i.e., in its local form) is expressed as

$$\varepsilon_{ijk}\sigma_{jk} = 0 \quad (3.5)$$

where ε_{ijk} is the permutation tensor. This ensures that the Cauchy stress tensor is symmetric (i.e., $\sigma_{jk} = \sigma_{kj}$).

Cosserat theory considers a continuum with a microstructure. It adds additional rotational degrees of freedom to the kinematics of the material points. In doing so, the rotations in the microstructure have to be balanced with couples in the equilibrium equations. In the case where there is a gradient in the couple (i.e., there is a rate of change in angular momentum) the Cauchy stress tensor can no longer be symmetric (i.e., $\sigma_{jk} \neq \sigma_{kj}$). The balance of linear momentum for a Cosserat continuum is the same as that of a traditional continuum. However, to accommodate the presence of couple stresses, the equilibrium equations in Cosserat theory include 9 couple stresses, μ_{ij} , which, summing over the moments for a differential element gives

$$\mu_{ji,j} + \varepsilon_{ijk}\sigma_{jk} = I\dot{\omega}_i. \quad (3.6)$$

Here, the couple stresses are torques per unit area, and are associated with the rotation of the material points. It can easily be shown in this case that if you have a net moment applied to the system, or a non-zero couple stress that isn't balanced by the net moment, that the stress tensor will not be symmetric.

In classical continuum theories, the stress tensor is required to be symmetric if moment equilibrium is to hold true. However, moment equilibrium is not present on the discrete scale in granular media. The hypothesis is that the slips that we see along the

shear bands are from particles attempting to rotate, building up a moment, and finally rotating. Once the particles rotate, that moment disappears. In visualizing the data, we can see which particles are building up a large moment and at what point the moment vanishes.

DEM Formulation

The study of shear banding spans multiple length scales. The motivation behind using micromechanical models to study shear banding is that the behavior of a soil sample (macroscale) is governed by the shear band, and the mechanics of the shear band are governed by the individual particles (microscale). Thus, a model that accounts for macroscale phenomena by calibrating only particle scale behavior is desirable for studying shear banding in granular media. DEM is used in this study because of its capability of producing such a model.

In this study, DEM simulations were carried out using a three-dimensional discrete element code. This is a non-commercial research code that was developed in house under a partnership between the United States Army Corps of Engineers Research and Development Center (ERDC) and Mississippi State University. In DEM, the particle physics are governed by the laws of motion and simple contact laws. The formulation (given by Peters et al. 2016) for the velocities (linear and rotational) are computed by integrating Newton's laws,

$$m \frac{\partial v_i}{\partial t} = m g n_i^g + \sum_{c=1}^N f_i^c \quad (3.7)$$

and

$$I_m \rho \frac{\partial w_k}{\partial t} = \sum_{c=1}^N \varepsilon_{ijk} f_i x_j + \sum_{c=1}^N m_k^c, \quad (3.8)$$

where m is the particle mass, I_m is the moment of inertia, gn_i^g is the acceleration due to gravity, and m_k^c is the contact moment. Notice the similarities between Equation 4.8 and Equation 4.6. Table 4.1 provides a summary of the relationship between DEM and Cosserat theory.

The contact laws that govern the particle interactions are given by equations 4.9 – 4.11.

$$f^n = \begin{cases} K^n \Delta^n \\ E_r K^n (\Delta^o - \Delta^n), & \Delta^n < \Delta^o \end{cases} \quad (3.9)$$

$$f_i^s = \begin{cases} K^s \Delta_i^s \\ f^n \tan \phi \, n_i^s, & |f_i^s| \geq f^n \tan \phi \end{cases} \quad (3.10)$$

and

$$m_i^c = \begin{cases} K^m \Delta \omega_i^c \\ f^n \tan \phi_m \, n_i^m, & |m_i^c| \geq f^n \tan \phi_m \end{cases} \quad (3.11)$$

where K^n and K^s are the normal and shear stiffness constants, respectively; E_r is the energy dissipation factor; Δ^n and Δ_i^s are the normal and shear components of the contact displacements; n_i^s and n_i^m are the unit vectors for the shear force and moment; Δ^o is the greatest value of penetration in the history of Δ^n ; and ϕ is the sliding friction and ϕ_m is the rolling friction parameters. These contact laws and the parameters used for them play an important role in the micromechanical behavior of the particles as well as the bulk response of the material. It is for the that reason that DEM is qualified as a proper tool for the study of instability due to shear banding.

The Antisymmetric stresses that arise out of Cosserat theory are a naturally emergent feature of the DEM particle assemblies. The particle definition of stress (see Peters et al. 2005) in DEM is well established and is defined as

$$\sigma_{ij}^p = \frac{1}{V^p} \sum_{c=1}^N f_i^c x_j^c \quad i, j = (1,2,3) \quad (3.12)$$

where V is the total solid volume of a particle, N the number of contacts for a particle, f_i^p is the contact force applied at the contact, and x_j^p is the spatial position (Figure 4.2).

Note, the p in the superscript denotes that the quantity is for a single particle, and the superscript c denotes a particular contact. The antisymmetric portion of the stress tensor is

$$\sigma_{ij}^{ap} = \frac{1}{2}(\sigma_{ij}^p - \sigma_{ji}^p) = \frac{1}{2} [\sum_c (f_i^c x_j^c - f_j^c x_i^c)] \quad (3.13)$$

The relationship between the antisymmetric component of the particle stress and the sum of the contact moments M_i on an individual particle, is seen clearly through expansion of the definition of the moment (cross product),

$$M_k = \sum_{c=1}^N \varepsilon_{ijk} f_i^c x_j^c. \quad (3.14)$$

where the summation from one to three on the indices is assumed and ε_{ijk} is the permutation tensor. Expanding equation 4.11 locally and dropping the summation symbol, we find

$$M_1 = f_2 x_3 - f_3 x_2$$

$$M_2 = f_3 x_1 - f_1 x_3$$

and

$$M_3 = f_1 x_2 - f_2 x_1.$$

Or, in general,

$$M_k = \sum_{c=1}^N f_i^c x_j^c - f_j^c x_i^c \quad (3.15)$$

Therefore, combining equations 4.13 and 4.15 and adding in the contact moments, the antisymmetric stresses are related to the moments by,

$$(\sigma_{ij}^p)^a = \frac{1}{2V^p} (M_k). \quad (3.16)$$

Rotation of particles in DEM occurs when the contact moments that resist rotation break down because a certain rolling resistance threshold is exceeded. Since particles must rotate to form shear bands, there could be some indicator through the antisymmetric stresses that a shear band is about to form. The purpose of this paper is to visualize the data from DEM simulations in such a way that the kinematics of the shear band can be qualified in such a way that can support future mathematical quantification.

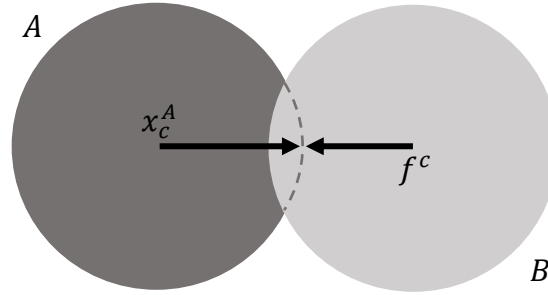


Figure 4.3 Particle contacts illustration for stress calculations.

Table 4.1 Bridging the scales: DEM and Cosserat Continuum

Variable	Discrete Element Method	Cosserat Continuum
Stress	f_i^c	σ_{ij}
Couples	m_i^c	μ_{ij}
Moments	$\varepsilon_{ijk} f_i^c x_j^c$	$\sigma_{ij} - \sigma_{ji}$
Linear Momentum Balance	$m \frac{\partial v_i}{\partial t} = f_i^g + \sum_{c=1}^N f_i^c$	$\rho \dot{v}_i = \rho b_i + \sigma_{ji,j}$
Angular Momentum Balance	$I_m \rho \frac{\partial \omega_k}{\partial t} = \sum_{c=1}^N \varepsilon_{ijk} f_i^c x_j^c + \sum_{c=1}^N m_k^c$	$I \dot{\omega}_i = \varepsilon_{ijk} \sigma_{jk} + \mu_{ji,j}$

Table 4.1 was adapted from personal communication with Peters (2017).

Methodology

For the purpose of studying the role of the antisymmetric stress in shear banding, three-dimensional, plane strain, discrete element simulations were performed to capture the kinematics of shear bands. Initialization of the simulations began with constructing an array of spheres (particles) of various radii within a specified size distribution were generated in three dimensions on a specified lattice as using the RANDOM_NUMBER function in FORTRAN 90. Figure 4.4 shows the assembly of particles consisting of 64000 particles with radii between 2.5 and 5.0 mm. The spheres were then isotopically consolidated without gravitational bias or friction until a small positive stress was measured at the boundaries. Several iterations of consolidation and energy dissipation was required to be able to maintain a small positive stress. Once the kinetic energy was sufficiently dissipated in the specimen, interparticle friction was applied and the system was loaded to a confining pressure of 55 kPa.

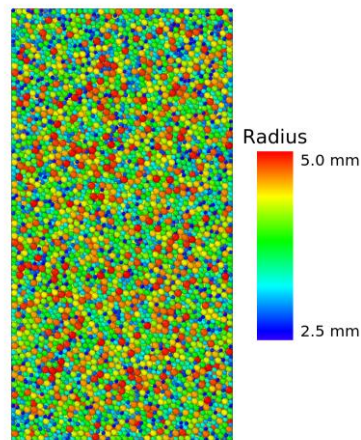


Figure 4.4 Distribution of particle sizes

The particle assembly if the initial plane strain configuration after isotropic consolidation. The radii of the particles are randomly distributed between 2.5 and 5.0 mm.

The particles in the simulations are, by necessity, larger than those of typical of laboratory testing of soils. Particle size can become an issue in the simulations when large rotation gradients are present, such as those observed in shear bands. This is accounted for by dimensional analysis which is used to ensure that similitude is maintained between the simulation and prototype scaling (Horner and Peters, 2000). Shear bands generally have a thickness of 10– 20 particles (Rice, 2006). thus, a simulation of a fully developed shear band would need to include the shear band plus the surrounding shear zone.

After initialization and confinement, a plane strain constant volume loading regime was applied to the sample. The initial geometry and relevant particle parameters used in the simulation are summarized in Table 3.1.

These parameters were chosen based on prior calibration performed by Goodman et al. (2017). The platens on the broad face of the specimen were kept in plane strain ($\varepsilon_x = 0$, where ε_x strain in the x -direction.), while the top and bottom platens compressed the specimen with a constant velocity. The y -platens were then adjusted at every DEM time step to ensure the change in volume throughout the simulation remains zero. Finally, the simulations were ran until a total axial strain, ε_z , of 15% was achieved.

From the plane strain simulations, three sample sizes where used to analyze the behavior of the system. First, the average behavior of the entire population of particles is considered. Second, a sample of only those particles that become part of the shear band

are studied. Finally, a sample of only those particles that are not a part of the shear band are examined.

Results and Discussion

Three cases were studied to see how the σ_{23}^a component of stress, out of plane rotation, out of plane contact moment, and particle porosity evolved throughout the constant volume simulation. The three cases are 1) the whole specimen consisting of 64000 particles, 2) the shear band only, and 3) outside the specimen, each consisting of 1000 particles. These three cases are illustrated in Figure 4.5.

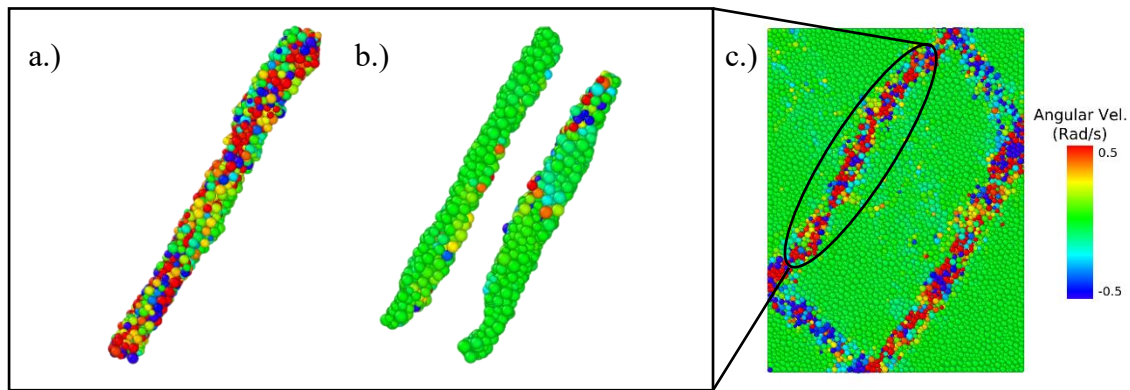


Figure 4.5 The three cases examined.

Illustration of the three cases examined: a.) the shear band only, b.) outside of the shear band, and c.) the whole specimen.

The cases a.) and b.) in Figure 4.5 were chosen by visual inspection of the angular velocities. That is, if the contours showed a significant angular velocity was considered as part of the shear band which implies a strong gradient of rotation across the shear band. The shear band begins to visually form at peak stress and at a strain of around

3.6%, and is fully developed by 5% strain. This is shown in the stress strain curve for the simulation (Figure 4.7).

Figure 4.6 provides further evidence for the hypothesis that the moments or antisymmetric stresses play a vital role in shear band formation. The snapshots in Figure 4.6 were made by holding all input parameters constant, and varying only rolling resistance. Each snapshot was taken at approximately 10% strain during the simulation, and the contours show the vertical component of the particle velocity. The rolling resistance applied to the spherical particles can be thought of as a Cosserat couple which contributes to the total moment (and therefore the antisymmetric stress) for each particle. If the rolling resistance factor is increased above a certain threshold, the moments in the particles do not allow the particles to rotate, and thus, no force chains break down and no shear band is able to form.

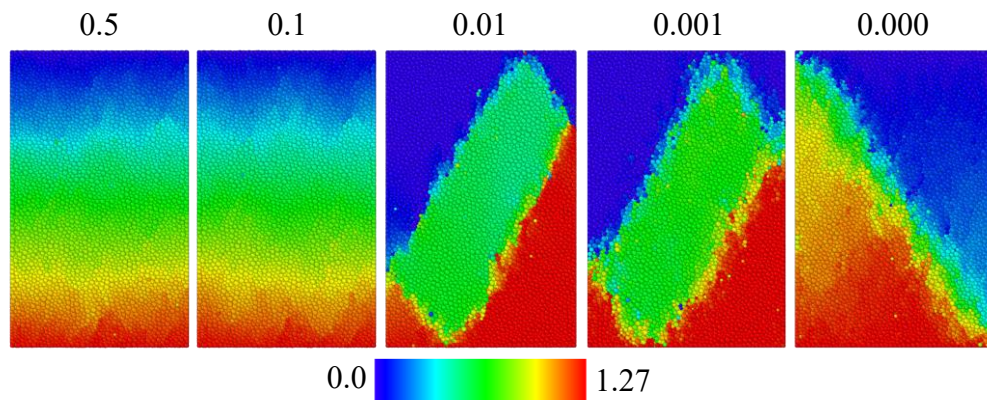


Figure 4.6 Shear band pattern and rolling resistance

Screenshots at 10% strain of the plane strain specimen at various values of rolling resistance as noted above each specimen. The colors represent velocity in the vertical direction.

In the case of no rolling resistance, there is nothing to keep the particles from rotating, and nothing to resist shear band formation. From this point of view, Figure 4.6 shows clearly that the shear band intersects the corner of the walls of the apparatus (platens not shown for clarity). Thus, it appears that the specimen geometry controls the shear band orientation when rolling resistance is zero.

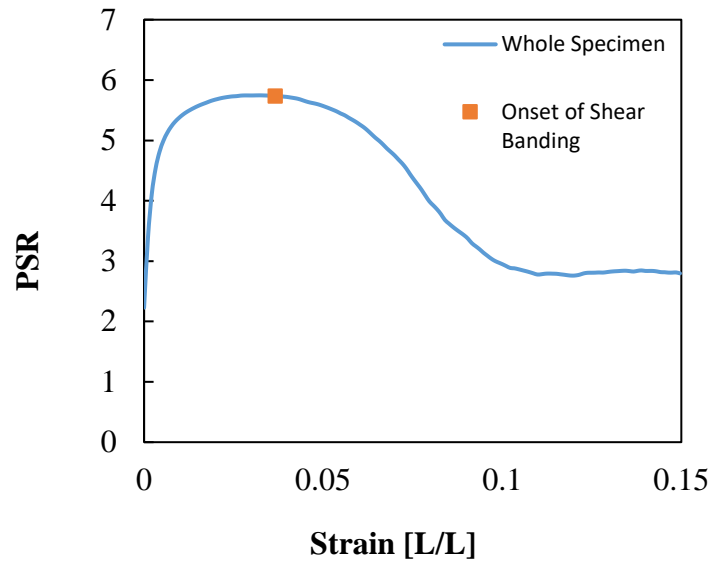


Figure 4.7 Stress – strain curve for the constant volume simulation

Stress-strain curve for the constant volume simulation with a marker indicating the onset of shear band formation at 3.6% strain.

The rotations of the individual particles were determined by examining the angular velocities of the particles. Figure 4.8 shows how the rotations vary as axial strain increases throughout the course of the simulation for the entire specimen. The rotations are initially scattered throughout the specimen, but localize in the shear band at a very early time in the stress-strain history. Once formed, the localized rotations carry on throughout the entirety of the simulation.

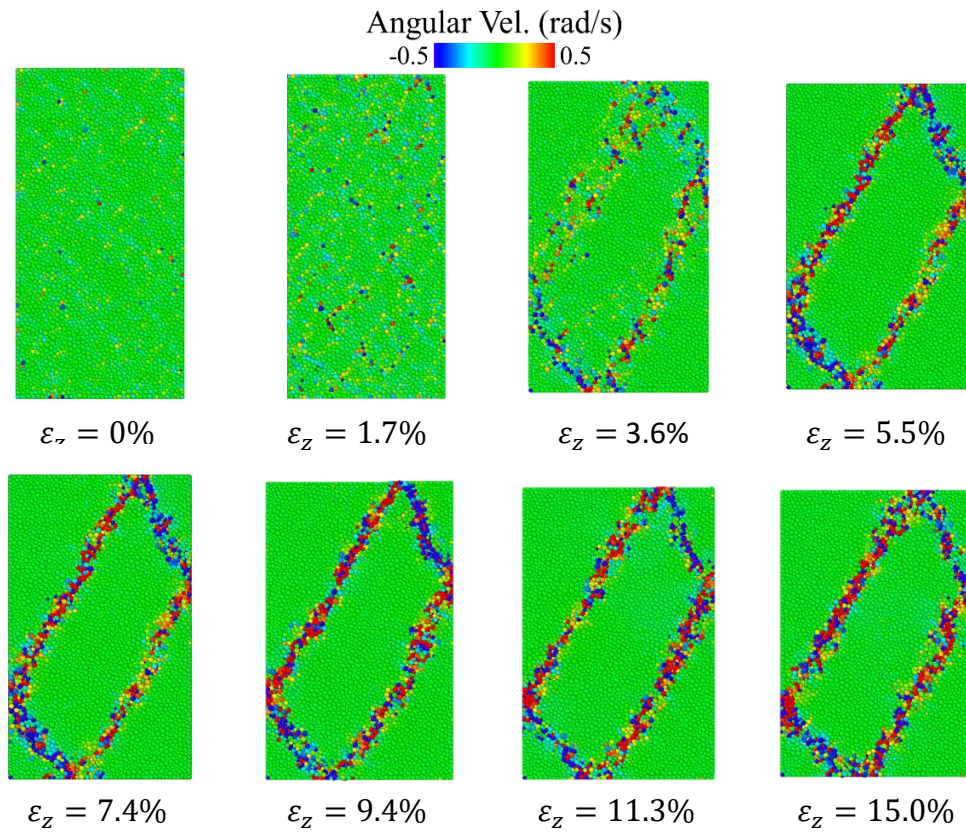


Figure 4.8 Angular velocity

Angular velocity of the particles, ω_x localizing into the shear band.

Figure 4.9 shows what is happening to the angular velocities as a function of strain for each of the three cases. For the entire specimen the average angular velocity remains fairly constant throughout the simulation. The particles outside of the band show similar behavior. Inside the band, however, the particle rotations spike, highlighting where all of the deformation is taking place. This increase in rotation in the shear band appears to come after shear band formation, indicating that the rotations are a result of the shear band formation rather than a cause of shear band formation.

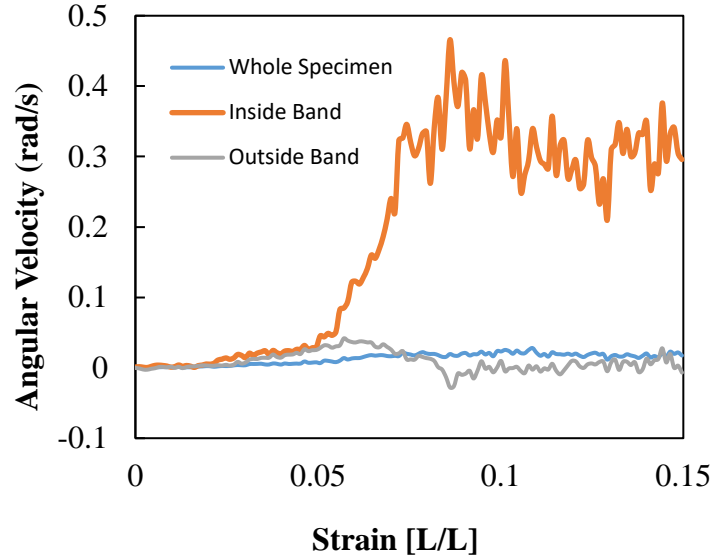


Figure 4.9 Average angular velocity for all three cases

Comparison of average angular velocity for each output time step for the three cases throughout the strain history of the specimen.

Figures 4.10 and 4.11 show the evolution of the contact moment (couples) for the particles. The average moment at each output time step oscillates about zero for the entirety of the simulation. After the shear band forms, bursts of moments are concentrated around the shear band, and highlight the location of the shear band similar to the rotation plots. The magnitudes of the oscillations begin to increase for all three cases after 5% strain (Figure 4.11). Like the rotations, the plots seem to indicate that the moments are affected by the shear band rather after formation rather than vice versa. It should be clarified reiterated that the contact moments are artificially introduced in the DEM to add a rolling resistance to the spherical particles. Although the couple moment is quite small in magnitude, its impact on the asymmetry of the stress tensor and impact on the microstructural behavior of the granular media is important (Oda and Iwashita 2000).

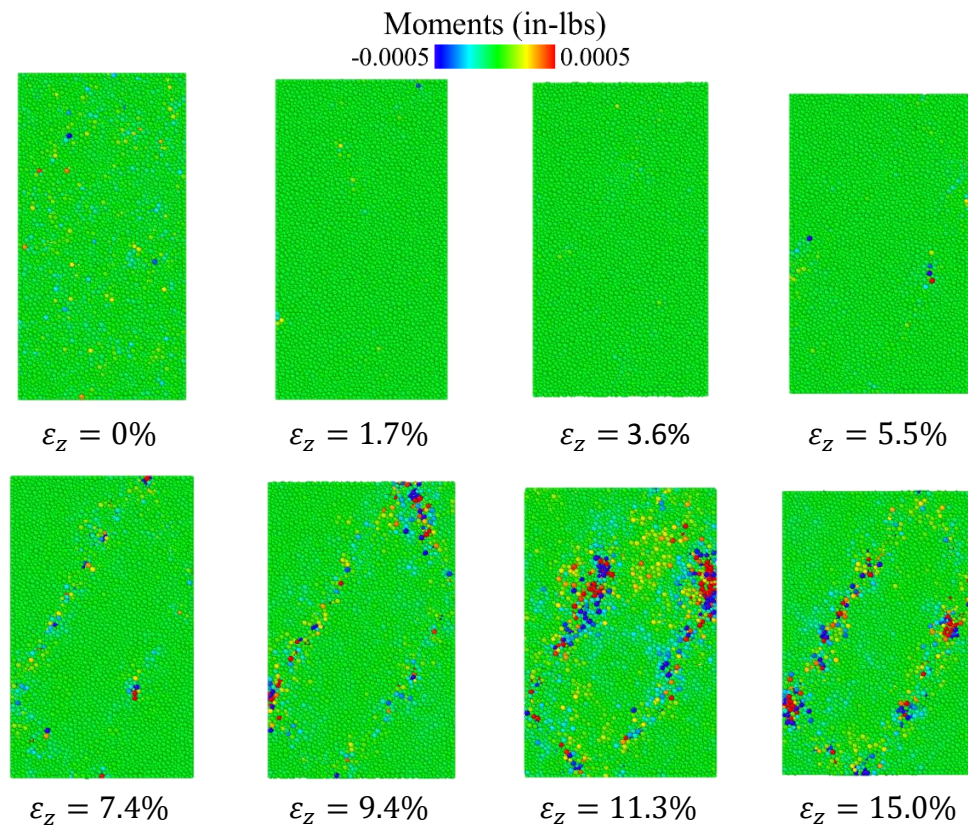


Figure 4.10 Particle contact moments

Particle contact moments, m_x at regular time intervals throughout the simulation.

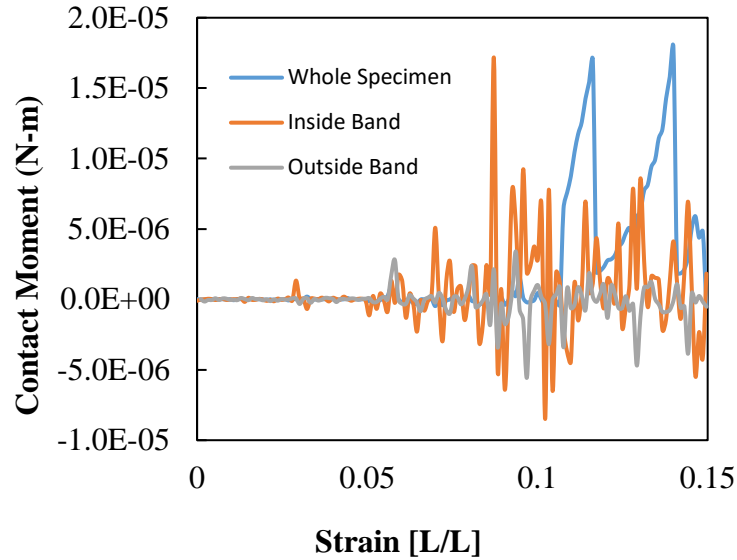


Figure 4.11 Average contact moments for all three cases

Comparison of the three cases for the contact moments throughout the strain history.

Figure 4.12 shows the evolution of the antisymmetric stress component σ_{23}^a throughout the simulation. Throughout the course of the simulation, the antisymmetric stress σ_{23}^a becomes increasingly non-zero because the contact moments/couples become significant. The other components of the antisymmetric stresses show similar patterns as Figure 4.12. Figure 4.13 shows that for each case, the antisymmetric stresses have an initially constant trend. Following shear band formation, the particles inside and outside of the shear band exhibit similar behavior and become increasingly positive as the simulation continues. It is difficult, based on the visualization techniques used here, to determine what portion of this behavior is attributed to the shear band formation.

Visualizations of the symmetric components of stress (not shown) shows similar behavior as the antisymmetric components.

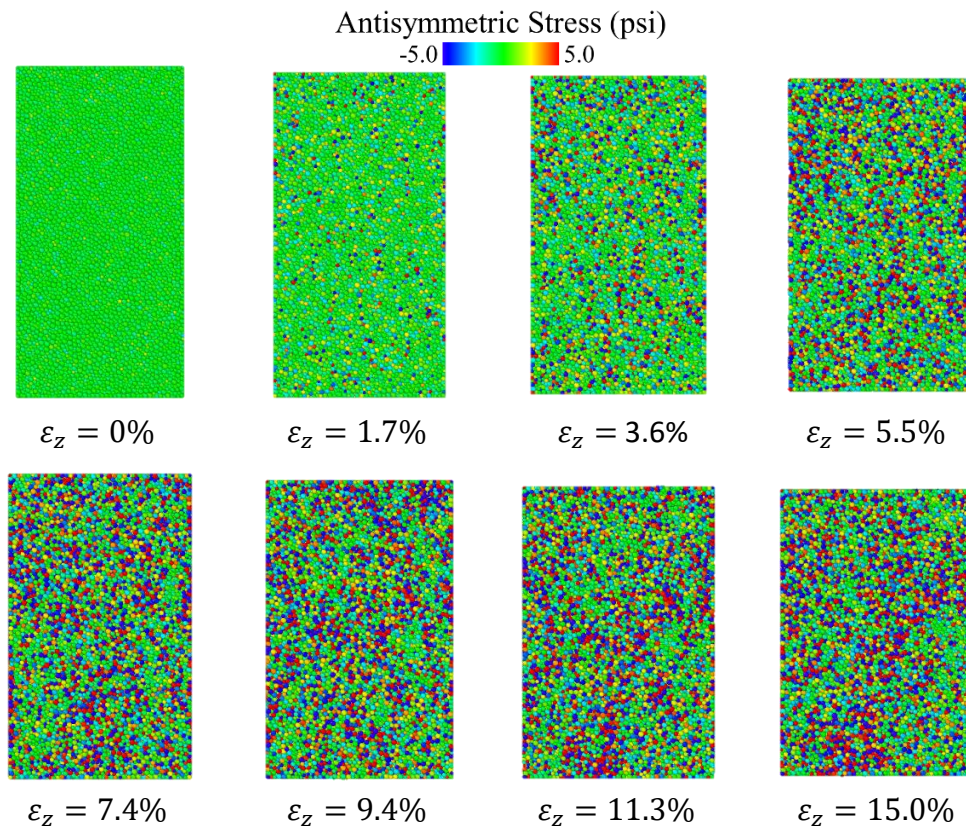


Figure 4.12 Antisymmetric stresses

Antisymmetric stresses σ_{23}^a for each particle at regular time increments throughout the simulation.

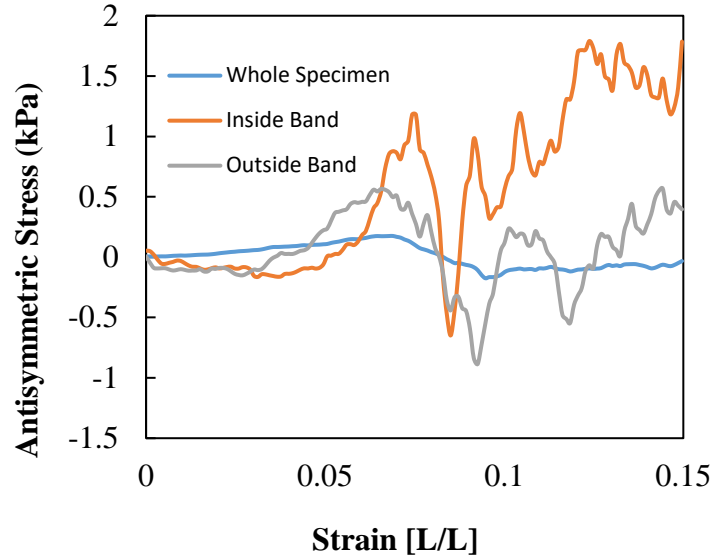


Figure 4.13 Average antisymmetric stress for all three cases

Comparison of the three cases for the antisymmetric stresses throughout the strain history.

The particle porosities in Figure 4.14 gives the porosity found using an algorithm which loops through all the spheres, specifies a spherical sampling volume (around each particle, and measures the solid fraction of the objects within that sphere. Note that the particles highlighted around the boundary are ignored because the high porosity is a boundary effect of the algorithm taking into account a portion around the sphere that has no solid fraction because it is outside of the boundary. Figure 4.15 shows that dilation occurs within the shear band, and the density increases outside of the shear band.

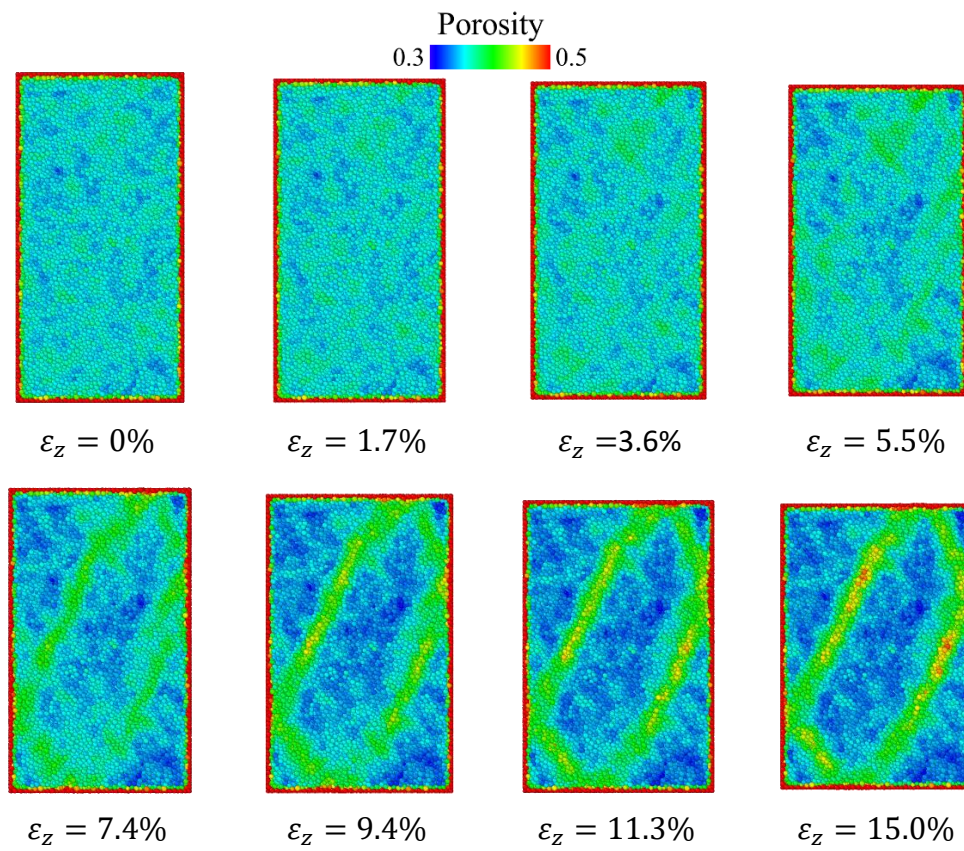


Figure 4.14 Local porosity

Local porosities show dilation after shear band formation.

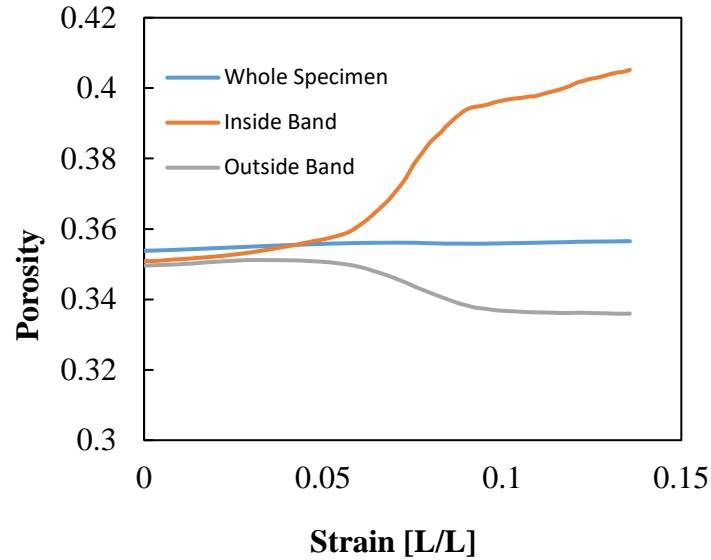


Figure 4.15 Average local porosity throughout the simulation

Comparison of the three cases for porosity throughout the strain history

One possible explanation of the results is that the output resolution of the simulation was not high enough to capture the effects of antisymmetric stresses on the shear bands. The output resolution for the constant volume simulation was 40 “frames” per second. That is, output data for every particle was gathered 40 times per simulation second. To test this, the same constant volume simulation was re-ran with an output resolution of 100 frames per second (data not show). Even at this resolution the results indicated that all activity for the variables involved occurred in the post-shear band stress-strain history. More resolution than that is feasible, but not practical.

One thing to note regarding the figures presented in this section, is that the shear bands are considered fully mobilized when rigid body displacement is present everywhere in the specimen except in the shear band. Figure 4.6 shows shear band formation in terms of the particle velocity, and it is clear that rigid body displacement is

occurring throughout the sections of the specimen separated by the shear band. The figures showing how the different measures evolve throughout the stress strain history of the specimen (particularly Figures 4.8 and 4.14) show that rigid body displacements are certainly not occurring inside the shear band.

Conclusions

Constant volume plane strain DEM simulations were performed to examine the relationship between shear band evolution and particle rolling, particle area porosity, contact moments, and antisymmetric stresses. 3 sampling cases were tested: 1) the entire particle population, 2) the shear band only, and 3) outside of the shear band. The antisymmetric stresses, in theory, were of interest as a possible indicator of shear band formation. Antisymmetric stress is a continuum concept that appears in micro-polar continua like Cosserat media, and is a naturally emergent feature of the DEM. It was hypothesized that the antisymmetric stresses would highlight the region where the shear band was going to form.

The qualitative and quantitative behavior of the antisymmetric stresses didn't appear to validate the hypothesis. Antisymmetric stresses, like rotations, moments, and particle porosity, appear to be effected by the shear band formation rather than the other way around. This finding demonstrates that the shear band may govern the constitutive response of the material rather than the constitutive response dictating the shear band. A better understanding of the mathematics of shear band formation, specifically, pre-shear band conditions is needed for better understanding of the actual constitutive behavior and the role that the shear band plays in the behavior and vice versa.

CHAPTER V CONCLUSIONS

Summary of Findings

This study used three dimensional, plane strain, discrete element simulations to study shear banding in granular media. Chapter 1 introduced the problem of shear banding and gave a broad overview of the thesis. Chapter 2 presented the necessary background information for studying shear banding in granular media. The two major methods of studying shear banding, bifurcation theory and micromechanics were also presented and discussed in their present context.

In chapter 3, a DEM model was developed and calibrated to simulate real sand. The calibration parameters showed a great sensitivity to rolling and sliding friction. Two different stress paths from two confining loading conditions, displacement- and force-controlled, were applied to the same reference assembly of particles. The results of the calibrated DEM specimen showed variation in shear band patterns and orientations under different loading conditions. These variations were similar to those found in physical laboratory testing performed on sand. This demonstrates the DEM simulation's ability to capture the potential mechanisms that drive shear band formation.

Chapter 4 presents a methodology and philosophy for studying the evolution of shear banding in soil, and relating it to continuum variables. In continuum mechanics, the stress tensor required to be symmetric if moment equilibrium is to hold true. However,

for each particle in our specimen moment equilibrium is not present on the discrete scale. This is evident from the presence of rotations that occur in physical and numerical simulations of laboratory tests on sand. Under homogeneous loading conditions, a continuum of particles should not have rotations. Not only are rotations present, but when the shear bands appear there are gradients in rotations. According to Cosserat theory, such gradients give rise to asymmetric terms in the stress tensor.

The hypothesis was that the slips that we see along the shear bands are from particles attempting to rotate, building up a moment, and finally rotating. Once the particles rotate, that moment disappears. In visualizing the high-resolution data, we could potentially see which particles are building up a large moment and at what point the moment vanishes. It was shown how these moments are related to the antisymmetric stresses. However, the hypothesis did not hold as expected. Visualizations of the data indicated that the antisymmetric stresses, moment, rotations, and porosities were all affected by the formation of the shear band rather than the other way around. This does not disprove the hypothesis, rather it indicates that our understanding of how the shear bands are formed is incomplete.

Recommendations for Further Research

In doing the research for this thesis, there are several items of business that call for further research and development. First, the need for improved visualization techniques for the study of shear banding is needed. Visualization is a vital tool for any numerical studies. It can also be a cumbersome task to develop user friendly and efficient visualization tools. Improved visualization techniques may include algorithms that are able to quickly identify which particles are a member of a shear band and extract data

specific to those particles. This would also be a useful tool for finding which particles were not members of a shear band and separately extracting those as well.

Another recommendation for further research is optimized calibration techniques for DEM modeling of granular media. All of the calibration done in this study was through trial and error. This is very time consuming and computationally expensive. Rackl and Hanley (2017) present a semi-automated and methodical method for calibrating DEM parameters using Latin hypercube sampling and kriging which appears promising. They are capable of optimizing the time step in the DEM as well as the 6 + parameters that need calibrating using their methodology. This optimizes computational efficiency as physical veracity in the DEM simulations. Further research in obtaining easy to use calibration techniques would improve research efficiency and effectiveness.

In addition to the calibration and visualization techniques, a study where a shear banding analysis done using Cosserat theory would be helpful. For this type of study, constitutive equations would need to be developed to utilize the continuum theory, and these would need to be tested under a variety of initial and boundary conditions. This could be implemented into typical continuum solvers such as a finite element code and would overcome the deficiencies of constitutive equations in classical continuum mechanics. However, prior to any study like this, the mathematics of localization would need to be developed, and DEM or other micromechanical analysis tools are promising for aiding in this task.

REFERENCES

- Alonso-Marroquin, F., & Vardoulakis, I. (2005). Micromechanics of shear bands in granular media. *Powders and grains*, 701-704.
- Alshibli, K. A., & Hasan, A. (2008). Spatial variation of void ratio and shear band thickness in sand using X-ray computed tomography. *Geotechnique*, 58(4), 249-257.
- Alshibli, K. A., & Sture, S. (2000). Shear band formation in plane strain experiments of sand. *Journal of Geotechnical and Geoenvironmental Engineering*, 126(6), 495-503.
- Bardet, J. P. (1990). A comprehensive review of strain localization in elastoplastic soils. *Computers and geotechnics*, 10(3), 163-188.
- Bardet, J. P., & Vardoulakis, I. (2001). The asymmetry of stress in granular media. *International Journal of Solids and Structures*, 38(2), 353-367.
- Batiste, S. N., Alshibli, K. A., Sture, S., & Lankton, M. (2004). Shear band characterization of triaxial sand specimens using computed tomography.
- Belheine, N., Plassiard, J. P., Donzé, F. V., Darve, F., & Seridi, A. (2009). Numerical simulation of drained triaxial test using 3D discrete element modeling. *Computers and Geotechnics*, 36(1), 320-331.
- Brodu, N., Dijksman, J. A., & Behringer, R. P. (2015). Spanning the scales of granular materials through microscopic force imaging. *Nature communications*, 6.
- Carrillo, A. R., Horner, D. A., Peters, J. F., & West, J. E. (1996, November). Design of a large scale discrete element soil model for high performance computing systems. In *Proceedings of the 1996 ACM/IEEE conference on Supercomputing* (p. 51). IEEE Computer Society.
- Coetzee, C. J. (2016). Calibration of the discrete element method and the effect of particle shape. *Powder Technology*, 297, 50-70.
- Cundall, P. A., & Strack, O. D. (1979). A discrete numerical model for granular assemblies. *Geotechnique*, 29(1), 47-65.
- Dantu, P. (1957). Contribution à l'étude mécanique et géométrique des milieux pulvérulents. Proc. 4th ICSMFE, London, 1957.

- Desrues, J., & Viggiani, G. (2004). Strain localization in sand: an overview of the experimental results obtained in Grenoble using stereophotogrammetry. *International Journal for Numerical and Analytical Methods in Geomechanics*, 28(4), 279-321.
- Donald, I. B., & Chen, Z. (1997). Slope stability analysis by the upper bound approach: fundamentals and methods. *Canadian Geotechnical Journal*, 34(6), 853-862
- Geer, S., Berger, J. R., Parnell, W. J., & Mustoe, G. G. W. (2017). A comparison of discrete element and micromechanical methods for determining the effective elastic properties of geomaterials. *Computers and Geotechnics*, 87, 1-9.
- Goldhirsch, I. (2010). Stress, stress asymmetry and couple stress: from discrete particles to continuous fields. *Granular Matter*, 12(3), 239-252.
- Goodman, C. C., Vahedifard, F., & Peters, J. F. Kinematics of Shear Banding in 3D Plane Strain DEM. In *Geotechnical Frontiers 2017* (pp. 519-528).
- Guo, N., & Zhao, J. (2016). 3D multiscale modeling of strain localization in granular media. *Computers and Geotechnics*, 80, 360-372.
- Heyman, J. (1972). Coulomb's memoir on statics: an essay in the history of civil engineering. CUP Archive.
- Hill, R. (1962). Acceleration waves in solids. *Journal of the Mechanics and Physics of Solids*, 10(1), 1-16.
- Hill, R. T. (1952). On discontinuous plastic states, with special reference to localized necking in thin sheets. *Journal of the Mechanics and Physics of Solids*, 1(1), 19-30.
- Horner, D. A., & Peters, J. F. (2000). Application of DEM to micro-mechanical theory for large deformations of granular media (No. ERDC/GL-TR-00-7). Engineer Research and Development Center Vicksburg, MS Geotechnical Lab.
- Horner, D. A., Peters, J. F., & Carrillo, A. (2001). Large scale discrete element modeling of vehicle-soil interaction. *Journal of engineering mechanics*, 127(10), 1027-1032.
- Iwashita, K., & Oda, M. (1998). Rolling resistance at contacts in simulation of shear band development by DEM. *Journal of engineering mechanics*, 124(3), 285-292.
- Iwashita, K., & Oda, M. (2000). Micro-deformation mechanism of shear banding process based on modified distinct element method. *Powder Technology*, 109(1), 192-205.

- Jing, X. Y., Zhou, W. H., Zhu, H. X., Yin, Z. Y., & Li, Y. (2017). Analysis of soil-structural interface behavior using three-dimensional DEM simulations. *International Journal for Numerical and Analytical Methods in Geomechanics*.
- Kuhn, M. R. (2003). Discussion of “The asymmetry of stress in granular media”:[JP Bardet and I. Vardoulakis, *Int. J. Solids Struct.* 2001, Vol. 38, No. 2, pp. 353–367]. *International journal of solids and structures*, 40(7), 1805-1807.
- Kuhn, M. R., Sun, W., & Wang, Q. (2015). Stress-induced anisotropy in granular materials: fabric, stiffness, and permeability. *Acta Geotechnica*, 10(4), 399-419.
- Lade, P. V., Van Dyck, E., & Rodriguez, N. M. (2014). Shear banding in torsion shear tests on cross-anisotropic deposits of fine Nevada sand. *Soils and Foundations*, 54(6), 1081-1093.
- Lade, P.V. & Wang, Q (2012). Method for Uniform Strain Extension Tests on Sand. *Geotechnical Testing Journal*, 35 (4), 1-11. Retrieved from <http://dx.doi.org/10.1520/GTJ103852>
- Laouafa, F., & Darve, F. (2002). Modelling of slope failure by a material instability mechanism. *Computers and Geotechnics*, 29(4), 301-325.
- Loukidis, D., & Ygeionomaki, N. (2017). Bearing Capacity in Sand Under Eccentric and Inclined Loading Using a Bounding Surface Plasticity Model. In *International Workshop on Bifurcation and Degradation in Geomaterials* (pp. 267-273). Springer, Cham.
- Ma, G., Zhou, W., Chang, X. L., Ng, T. T., & Yang, L. F. (2016). Formation of shear bands in crushable and irregularly shaped granular materials and the associated microstructural evolution. *Powder Technology*, 301, 118-130.
- Maciejewski, J., & Jarzębowski, A. (2002). Laboratory optimization of the soil digging process. *Journal of Terramechanics*, 39(3), 161-179.
- Marone, C., & Kilgore, B. (1993). Scaling of the critical slip distance for seismic faulting with shear strain in fault zones. *Nature*, 362(6421), 618-621.
- Mohr, O. (1900). Welche Umstände bedingen die Elastizitätsgrenze und den Bruch eines Materials. *Zeitschrift des Vereins Deutscher Ingenieure*, 46(1524-1530), 1572-1577.
- Mühlhaus, H. B., & Vardoulakis, I. (1987). The thickness of shear bands in granular materials. *Geotechnique*, 37(3), 271-283.

- Ngo, N. T., Indraratna, B., & Rujikiatkamjorn, C. (2016). Micromechanics-based investigation of fouled ballast using large-scale triaxial tests and discrete element modeling. *Journal of Geotechnical and Geoenvironmental Engineering*, 143(2), 04016089.
- Oda, M. (1972). The mechanism of fabric changes during compressional deformation of sand. *Soils and foundations*, 12(2), 1-18.
- Oda, M., & Iwashita, K. (2000). Study on couple stress and shear band development in granular media based on numerical simulation analyses. *International journal of engineering science*, 38(15), 1713-1740.
- Oda, M., & Kazama, H. (1998). Microstructure of shear bands and its relation to the mechanisms of dilatancy and failure of dense granular soils. *Geotechnique*, 48(4), 465-481.
- Oda, M., Koishikawa, I., & Higuchi, T. (1978). Experimental study of anisotropic shear strength of sand by plane strain test. *Soils and foundations*, 18(1), 25-38.
- Oda, M., Takemura, T., & Takahashi, M. (2004). Microstructure in shear band observed by microfocus X-ray computed tomography. *Geotechnique*, 54(8), 539-542.
- O'Sullivan, C. (2011). *Particulate discrete element modelling: a geomechanics perspective*. Taylor & Francis.
- Peters, J. F. (2005). Some fundamental aspects of the continuumization problem in granular media. In *Mathematics and Mechanics of Granular Materials* (pp. 231-250). Springer Netherlands.
- Peters, J.F. (2017) Personal communication.
- Peters, J. F., Carrillo, A. R., Vahedifard, F., Jelinek, B., Goodman, C. C., Johnson, D. H., & Fili, J. F., (2016) Development of a Virtual Terrain for Mobility Analysis. Internal Report.
- Peters, J. F., & Walizer, L. E. (2013). Patterned nonaffine motion in granular media. *Journal of Engineering Mechanics*, 139(10), 1479-1490.
- Peters, J. F., Lade, P. V., & Bro, A. (1988). Shear band formation in triaxial and plane strain tests. In *Advanced triaxial testing of soil and rock*. ASTM International.
- Peters, J. F., Muthuswamy, M., Wibowo, J., & Tordesillas, A. (2005). Characterization of force chains in granular material. *Physical review E*, 72(4), 041307.
- Rackl, M., & Hanley, K. J. (2017). A methodical calibration procedure for discrete element models. *Powder Technology*, 307, 73-83.

- Radjai, F., Roux, J. N., & Daouadji, A. (2017). Modeling Granular Materials: Century-Long Research across Scales. *Journal of Engineering Mechanics*, 143(4), 04017002.
- Rechenmacher, A. L. (2006). Grain-scale processes governing shear band initiation and evolution in sands. *Journal of the Mechanics and Physics of Solids*, 54(1), 22-45.
- Rechenmacher, A. L., & Finno, R. J. (2003). Digital image correlation to evaluate shear banding in dilative sands.
- Rice, J. R. (1973). Plasticity and soil mechanics. In *Proc. of the symposium of the role of plasticity in soil mechanics*, Cambridge/UK (p. 263).
- Rice, J. R. (1976). The localization of plastic deformation. *Proceedings Theoretical and Applied Mech.* (207-220)
- Rice, J. R. (2006). Heating and weakening of faults during earthquake slip. *Journal of Geophysical Research: Solid Earth*, 111(B5).
- Rudnicki, J and Rice, J. (1975). Conditions for the localization of deformation in pressure-sensitive dilatant materials. *J. of the Mechs. and Physics of solids* 23(6).
- Saadatfar, M., Sheppard, A. P., Senden, T. J., & Kabla, A. J. (2012). Mapping forces in a 3D elastic assembly of grains. *Journal of the Mechanics and Physics of Solids*, 60(1), 55-66.
- Sadrekarimi, A., & Olson, S. M. (2009). Shear band formation observed in ring shear tests on sandy soils. *Journal of geotechnical and geoenvironmental engineering*, 136(2), 366-375.
- Senatore, C., & Iagnemma, K. (2014). Analysis of stress distributions under lightweight wheeled vehicles. *Journal of Terramechanics*, 51, 1-17.
- Senatore, C., Wulfmeier, M., Vlahinić, I., Andrade, J., & Iagnemma, K. (2013). Design and implementation of a particle image velocimetry method for analysis of running gear–soil interaction. *Journal of Terramechanics*, 50(5), 311-326.
- Shi, B., Murakami, Y., Wu, Z., Chen, J., & Inyang, H. (1999). Monitoring of internal failure evolution in soils using computerization X-ray tomography. *Engineering Geology*, 54(3), 321-328.
- Thomas, T. Y. (1961). *Plastic Flow and Fracture in Solids by Tracy Y Thomas* (Vol. 2). Elsevier.
- Tordesillas, A. (2007). Force chain buckling, unjamming transitions and shear banding in dense granular assemblies. *Philosophical Magazine*, 87(32), 4987-5016.

- Tordesillas, A., & Muthuswamy, M. (2009). On the modeling of confined buckling of force chains. *Journal of the Mechanics and Physics of Solids*, 57(4), 706-727.
- Tordesillas, A., Peters, J. F., & Gardiner, B. S. (2004). Shear band evolution and accumulated microstructural development in Cosserat media. *International Journal for Numerical and Analytical Methods in Geomechanics*, 28(10), 981-1010.
- Tordesillas, A., Pucilowski, S., Walker, D. M., Peters, J. F., & Walizer, L. E. (2014). Micromechanics of vortices in granular media: connection to shear bands and implications for continuum modelling of failure in geomaterials. *International Journal for Numerical and Analytical Methods in Geomechanics*, 38(12), 1247-1275.
- Tordesillas, A., & Walsh, D. S. (2002). Incorporating rolling resistance and contact anisotropy in micromechanical models of granular media. *Powder Technology*, 124(1), 106-111.
- Valanis, K., Peters, J. F., & Gill, J. (1993). Configurational entropy, non-associativity and uniqueness in granular media. *Acta Mechanica*, 100(1-2), 79-93.
- Valanis, K. C., & Peters, J. F. (1996). Ill-posedness of the initial and boundary value problems in non-associative plasticity. *Acta mechanica*, 114(1), 1-25.
- Van Asch, T. W., Van Beek, L. P. H., & Bogaard, T. A. (2007). Problems in predicting the mobility of slow-moving landslides. *Engineering geology*, 91(1), 46-55.
- Vardoulakis, I. (1980). Shear band inclination and shear modulus of sand in biaxial tests. *Int'l J. for Num. and Analytical Methods in Geomech.*, 4(2), 103-119.
- Vardoulakis, I., & Sulem, J. (1995). *Bifurcation analysis in geomechanics*. Chapman & Hall
- Vardoulakis, I., Goldscheider, M., & Gudehus, G. (1978). Formation of shear bands in sand bodies as a bifurcation problem. *Int'l J. for Num. and Analytical Methods in Geomech.*, 2(2), 99-128.
- Wakabayashi, T. (1950). Photo-elastic method for determination of stress in powdered mass. *Journal of the Physical Society of Japan*, 5(5), 383-385.
- Walsh, S. D., Tordesillas, A., & Peters, J. F. (2007). Development of micromechanical models for granular media. *Granular Matter*, 9(5), 337-352
- Wang, Q., & Lade, P. V. (2001). Shear banding in true triaxial tests and its effect on failure in sand. *Journal of Engineering Mechanics*, 127(8), 754-761.

- Wang, B., Vardon, P. J., & Hicks, M. A. (2016). Investigation of retrogressive and progressive slope failure mechanisms using the material point method. *Computers and Geotechnics*, 78, 88-98.
- Wolf, H., König, D., & Triantafyllidis, T. (2003). Experimental investigation of shear band patterns in granular material. *Journal of Structural Geology*, 25(8), 1229-1240.
- Zhao, J., & Guo, N. (2013). Unique critical state characteristics in granular media considering fabric anisotropy. *Géotechnique*, 63(8), 695.
- Zhou, W., Yang, L., Ma, G., Xu, K., Lai, Z., & Chang, X. (2017). DEM modeling of shear bands in crushable and irregularly shaped granular materials. *Granular Matter*, 19(2), 25.